AD-A141 038 ELECTRON EXCITATION OF VIBRATIONAL STATES OF D2 AND H2 AND DETECTION OF E.. (U) NATIONAL BUREAU OF STANDARDS BOULDER CO QUANTUM PHYSICS DIV A V PHELPS ET AL. 1/1

UNCLASSIFIED APR 84 AFWAL-TR-84-2017 F/G 7/4 NL

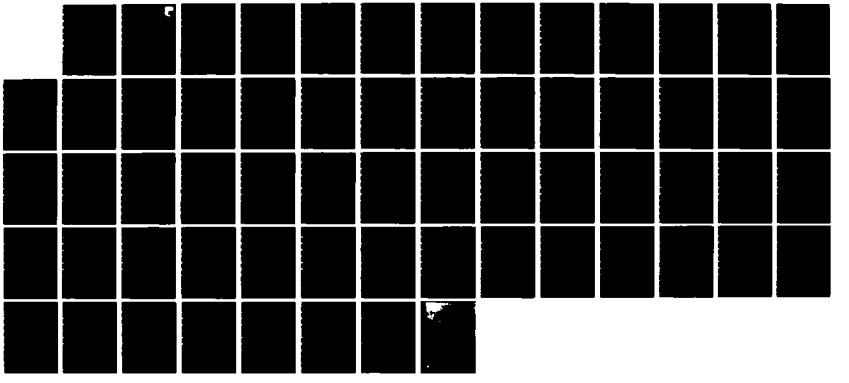

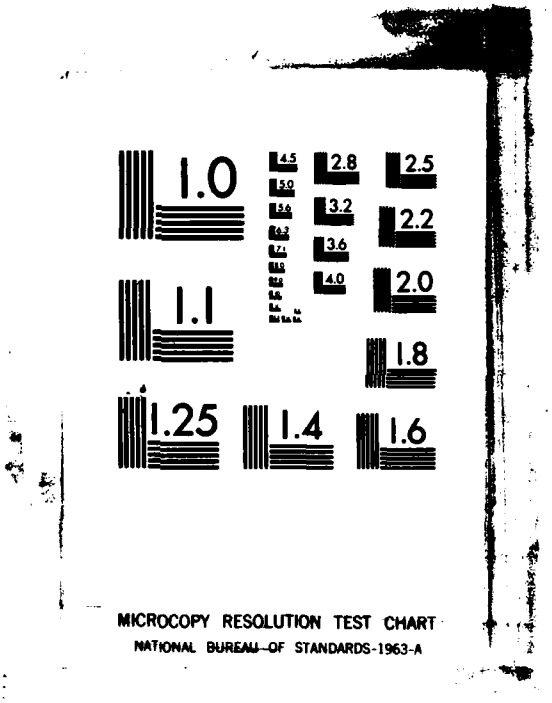
1.0
1.1
1.25
1.4
1.6
1.8
2.0
2.2
2.5
2.8
3.2
3.6
4.0
4.5
5.0
5.6
MICROCOPY RESOLUTION TEST CHART
NATIONAL BUREAU OF STANDARDS-1963-A

AFWAL-TR-84-2017

ELECTRON EXCITATION OF VIBRATIONAL STATES OF D_2 AND H_2 AND DETECTION OF EXCITED STATES BY LASER-INDUCED FLUORESCENCE

A. V. PHELPS
S. J. BUCKMAN
H. TISCHER

QUANTUM PHYSICS DIVISION
U.S. BUREAU OF STANDARDS
BOULDER, CO 80303

April 1984

FINAL REPORT FOR PERIOD OCTOBER 1982 - SEPTEMBER 1983

Approved for public release; distribution unlimited

AERO PROPULSION LABORATORY
AIR FORCE WRIGHT AERONAUTICAL LABORATORIES
AIR FORCE SYSTEMS COMMAND
WRIGHT-PATTERSON AIR FORCE BASE, OHIO 45433

NOTICE

When Government drawings, specifications, or other data are used for any purpose other than in connection with a definitely related Government procurement operation, the United States Government thereby incurs no responsibility nor any obligation whatsoever; and the fact that the government may have formulated, furnished, or in any way supplied the said drawings, specifications, or other data, is not to be regarded by implication or otherwise as in any manner licensing the holder or any other person or corporation, or conveying any rights or permission to manufacture use, or sell any patented invention that may in any way be related thereto.

This report has been reviewed by the Office of Public Affairs (ASD/PA) and is releasable to the National Technical Information Service (NTIS). At NTIS, it will be available to the general public, including foreign nations.

This technical report has been reviewed and is approved for publication.

ALAN GARSCADDEN
Project Engineer

PAUL R. BERTHEAUD
Chief, Energy Conversion Branch
Aerospace Power Division
Aero Propulsion Laboratory

FOR THE COMMANDER

JAMES D. REAMS
Chief, Aerospace Power Division
Aero Propulsion Laboratory

"If your address has changed, if you wish to be removed from our mailing list, or if the addressee is no longer employed by your organization please notify AFWAL/POOC, *W-PAFB, OH 45433 to help us maintain a current mailing list".*

Copies of this report should not be returned unless return is required by security considerations, contractual obligations, or notice on a specific document.

Unclassified

SECURITY CLASSIFICATION OF THIS PAGE (When Data Entered)

REPORT DOCUMENTATION PAGE		READ INSTRUCTIONS BEFORE COMPLETING FORM
1. REPORT NUMBER AFWAL-TR-84-2017	2. GOVT ACCESSION NO. A141038	3. RECIPIENT'S CATALOG NUMBER
4. TITLE (and Subtitle) Electron Excitation of Vibrational States of D_2 and H_2, and Detection of Excited States by Laser Induced Fluorescence		5. TYPE OF REPORT & PERIOD COVERED Final Report for Period Oct 82 - Sep 83 6. PERFORMING ORG. REPORT NUMBER
7. AUTHOR(s) A. V. Phelps, S. J. Buckman, and H. Tischer		8. CONTRACT OR GRANT NUMBER(s) MIPR FY1455-82-N0635 MIPR FY1455-83-N0621
9. PERFORMING ORGANIZATION NAME AND ADDRESS Quantum Physics Division U.S. Bureau of Standards Boulder, CO 80303		10. PROGRAM ELEMENT, PROJECT, TASK AREA & WORK UNIT NUMBERS 2301S124
11. CONTROLLING OFFICE NAME AND ADDRESS Aero Propulsion Laboratory (AFWAL/POOC) Air Force Wright Aeronautical Laboratories (AFSC) Wright-Patterson Air Force Base, Ohio 45433		12. REPORT DATE April 1984 13. NUMBER OF PAGES 60
14. MONITORING AGENCY NAME & ADDRESS (if different from Controlling Office)		15. SECURITY CLASS. (of this report) Unclassified 15a. DECLASSIFICATION DOWNGRADING SCHEDULE

16. DISTRIBUTION STATEMENT (of this Report)

Approved for public release; distribution unlimited.

17. DISTRIBUTION STATEMENT (of the abstract entered in Block 20, if different from Report)

18. SUPPLEMENTARY NOTES

19. KEY WORDS (Continue on reverse side if necessary and identify by block number)

hydrogen, electrons, radiation, excitation coefficient, vibration, infrared, fluorescence, excited states, carbon monoxide, carbon dioxide, excitation transfer

20. ABSTRACT (Continue on reverse side if necessary and identify by block number)

Measurements and analyses are reported for the vibrational excitation of D_2 and H_2 by low and moderate energy electrons. The measurements were made using the electron drift tube technique. The vibrationally excited D_2 and H_2 are detected by the transfer of excitation to CO or CO_2 and the measurement of the intensity of 4.7μm or 4.3μm infrared emission. The derived cross sections for the vibrational excitation of D_2 are significantly smaller than the corresponding cross sections for H_2. Apparatus has been constructed and tested for the measurement of the density of excited H_2 in the $c^3\Pi_u$ metastable state by laser induced fluorescence and laser absorption techniques.

DD FORM 1 JAN 73 1473 EDITION OF 1 NOV 65 IS OBSOLETE

Unclassified

SECURITY CLASSIFICATION OF THIS PAGE (When Data Entered)

PREFACE

This work was performed in the Quantum Physics Division, U.S. Bureau of Standards, at the Joint Institute for Laboratory Astrophysics under MIPR FY1455-82-N0635 and MIPR FY1455-83-N0621. This work was performed during the period October 1982 through September 1983 under Project 2301 Task S1, Work Unit 24. The Air Force contract manager was Dr. Alan Garscadden, Energy Conversion Branch, Aero Propulsion Laboratory, WPAFB, OH 45433.

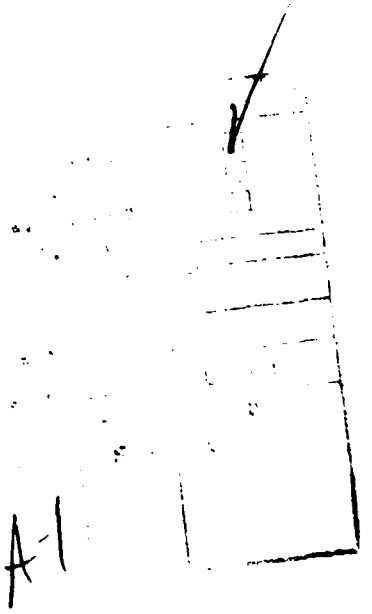

TABLE OF CONTENTS

LIST OF ILLUSTRATIONS

FIGURE PAGE

LIST OF TABLES

SECTION I

INTRODUCTION

The measurements and analyses described in this report are concerned with the development and application of techniques for the determination of densities of excited molecules and rates of production and loss of excited molecules in electric discharge systems. Electrical discharges in molecular gases, such as H_2 and D_2, are the subject of renewed interest because of their importance in devices such as high power switches, plasma processing cells and negative ion sources and because of the need for improved performance of these devices. In addition, the physical process, such as metastable formation and quenching, being measured under this project for H_2, are also of importance in atmospheric gases where current interest is in phenomena such as charged particle beam propagation and lightning.

In Section II of this report we describe our measurements of the vibrational excitation of D_2 and H_2. In these experiments we make use of the process of excitation transfer from the D_2 or H_2 to small concentrations of either CO_2 or CO and then observe the infrared emission from the CO_2 or CO. The infrared emission from N_2-CO_2 and N_2-CO mixture is used to calibrate the detection system. We first review briefly the experimental technique and the corrections to be made to the measured infrared signals for the absorption by the CO_2 or CO and for the effects of ionization on the measured currents. Then for each

gas mixture we review the available kinetics data and present our excitation coefficient results.

Section III of this report contains a description of work carried out during this contract period on the development and application of techniques for the measurement of excited state densities in gas discharge devices. In particular, we have made measurements of the collisional quenching of the $a^3\Sigma_g^+$ state of H_2 using our drift tube technique and built and tested apparatus for the measurement of laser-induced fluorescence and absorption by the $c^3\Pi_u$ metastable state of H_2.

Section IV contains the conclusions based on this research.

SECTION II

VIBRATIONAL EXCITATION OF D_2 AND H_2 BY ELECTRONS

1. INTRODUCTION

Interest in the vibrational excitation of D_2 and H_2 by electrons arises from the importance of these molecules as the working media in gas discharge switches (Reference 1) and negative ion sources (Reference 2) as well as from their importance as test cases for the comparison of theory and experiment (References 3-4). Although considerable data are available on the vibrational excitation of H_2 (References 3, 5,6), there is disagreement as to the behavior of the excitation cross section near threshold. Very little cross section information is available on the vibrational excitation of D_2 (References 7-9), and some of it is believed to be in error especially at the higher energies (Reference 7). The research described in this report was undertaken in order to develop and apply techniques for the measurement of excitation coefficients and the determination of cross sections for the vibrational excitation of D_2 and H_2 by low-energy electrons. The general technique used is to excite the D_2 or H_2 in an electron drift tube, to allow some of the excitation to transfer to an infrared emitting molecule such as CO or CO_2, and to measure the intensity of the infrared emission. Since the drift tube and infrared measurement techniques have been described in great detail in our publications (References 10,11), we will not discuss them in detail in this report.

After a discussion of the model used to interpret our data, we present the results of our analysis of the experimental measurements of vibrational excitation of D_2 and H_2 carried out during late 1982. In these experiments 0.1 to 2% CO_2 or CO was added to the D_2 or H_2 and measurements were made of the absolute intensity of emission at 4.3 or 4.7 μm resulting from V-V transfer from the D_2 or H_2 to the carbon containing molecule. In addition, measurements were made of the emission from mixtures of N_2 and 0.02 to 4% of either CO_2 or CO. These data provide a basis for normalization of the absolute intensity measurements, since it is known that over a range of E/n for nearly pure N_2 95±3% of the available electron energy results in vibrational excitation of N_2. For each gas combination we will first summarize the relevant collisional kinetics and our decay constant measurements. Then, we will discuss our experimental and theoretical results for the absolute vibrational excitation coefficients.

2. MODEL OF EXPERIMENT

a. Rate equations and excitation coefficient

Here we summarize the equations used to analyze our experimental data. We assume that the reader is familiar with the models of our experiment given in detail by Bulos and Phelps (Reference 10) and Lawton and Phelps (Reference 11).

The equations which describe the density of vibrationally excited molecules have been discussed by a number of authors (References 12-14). If we indicate the density of vibrationally excited D_2, H_2, or N_2 by $X^{\ddagger}$ and the density of vibrationally excited CO or of CO_2 in the

001 mode by $C^{\ddagger}$, then rate equations are:

$$\frac{dX^{\ddagger}}{dt} = -\nu_X X^{\ddagger} + \nu_{CX} C^{\ddagger} + \alpha_{eX} W n_e \quad , \tag{1}$$

and

$$\frac{dC^{\ddagger}}{dt} = +\nu_{XC} X^{\ddagger} - \nu_C C^{\ddagger} + \alpha_{eC} W n_e \quad . \tag{2}$$

Here ν_X and ν_C are the frequencies of destruction of $X^{\ddagger}$ and $C^{\ddagger}$ including excitation transfer; ν_{XC} and ν_{CX} are the frequencies of excitation transfer collisions from $X^{\ddagger}$ to $C^{\ddagger}$ and the reverse; α_{eX} and α_{eC} are the coefficients for electron excitation of $X^{\ddagger}$ and $C^{\ddagger}$, respectively, and n_e and W are the electron density and drift velocity. The destruction frequencies are given by

$$\nu_X = \frac{D(X^{\ddagger})n}{n\Lambda^2} + \left[k_{XX}^{VT}(1-X_C) + k_{XC}^{VT}X_C + k_{XC}^{VV}X_C\right] n \quad , \tag{3}$$

and

$$\nu_C = \frac{D(C^{\ddagger})n}{n\Lambda^2} + \left[k_{CC}^{VT}X_C + k_{CX}^{VT}(1-X_C) + k_{CX}^{VV}(1-X_C)\right] n \quad . \tag{4}$$

Here $D(X^{\ddagger})n$ and $D(C^{\ddagger})n$ are the diffusion coefficients at unit density for $X^{\ddagger}$ and $C^{\ddagger}$ molecules in the gas mixture used, Λ is the diffusion length for the fundamental diffusion mode, X_C is the fractional concentration of carbon containing molecules and k_{XX}^{VT} and k_{XC}^{VT} are the rate coefficients for the VT quenching of $X^{\ddagger}$ by ground state X molecules and C molecules, respectively. Similarly, k_{CC}^{VT} and k_{CX}^{VT} are the VT quenching rate coefficients for $C^{\ddagger}$ by ground state C and X molecules. The rate coefficients k_{XC}^{VV} and k_{CX}^{VV} describe the transfer of excitation

from $X^{\ddagger}$ to $C^{\ddagger}$ and the reverse reaction. The values of the rate coefficients and diffusion coefficients used in the analyses of this report are given in Table 1. We assume that the diffusion length is given by $\Lambda = L/\pi = 1.22E \times 10^{-2}$ m for these experiments (Reference 11). Also, we assume that the loss of excitation by the escape of radiation is described by Holstein's (Reference 15) fundamental mode, i.e., by gA, where g is taken to be equal to the value of the fractional transmission at a distance equal to the electrode separation L.

The solution to Eqs. (1) and (2) for the density of excited carbon containing molecules at gas densities which are high enough so that diffusion effects are small is

$$C^{\ddagger}(t) = \frac{W\, n_e n}{\nu_S \nu_F (\nu_F - \nu_S)} \left\{ \frac{\alpha_{eN}}{n} \nu_{XC} \left[\nu_F \left(1 - e^{-\nu_S t}\right) - \nu_S \left(1 - e^{-\nu_F t}\right) \right] \right.$$

$$\left. + \frac{\alpha_{eC}}{n} \left[\nu_F (\nu_X - \nu_S) \left(1 - e^{-\nu_S t}\right) + \nu_S (\nu_F - \nu_X) \left(1 - e^{-\nu_F t}\right) \right] \right\} , \tag{5}$$

where

$$\nu_F, \nu_S = \frac{(\nu_X + \nu_C)}{2} \pm \left[\frac{(\nu_X + \nu_C)}{4} - \nu_X \nu_C + \nu_{XC} \nu_{CX} \right]^{1/2} . \tag{6}$$

Here ν_S is the decay constant associated with the slower varying component of the two exponentials in Eq. (5) and is the decay constant determined by fitting our experimental data. The decay constant associated with the faster exponential ν_F was measured in only a few of our experiments and, therefore, was determined from other experiments as discussed later.

Table 1. Rate coefficients used in analyses of infrared emission data.

X	C	(Dn) $m^{-1}\ s^{-1}$	k^{VT}_{XX} m^3/s	k^{VV}_{XC} m^3/s	k^{VV}_{CX} m^3/s	k^{VT}_{CC} m^3/s	k^{VT}_{XC} m^3/s	k^{VT}_{CX} m^3/s	A s^{-1}
N_2	CO_2	3(24)*	1(-25)	5.14(-19)	5.6(-19)	1.1(-20)	0†	3.3(-21)	460
D_2	CO_2	1(25)	2(-23)	3.3(-19)	1.5(-20)	1.1(-20)	0†	1.1(-20)	460
H_2	CO_2	1.5(25)	2(-22)	2(-20)	3.4(-24)	1.1(-20)	6(-24)	1.2(-19)	460
N_2	CO	4(24)	1(-25)	1.43(-20)	5.7(-21)	4(-26)	0†	1(-24)	33.4
D_2	CO	8(24)	2(-23)	5.6(-21)	9.6(-23)	4(-26)	0†	1.35(-23)	33.4
H_2	CO	1.5(25)	2.75(-25)	3.8(-22)	4.2(-26)	2.3(-26)	0†	4.4(-22)	33.4

*3(24) means 3×10^{24}.

† k^{VT}_{XC} was set equal to zero because of the lack of information and the lack of sensitivity of our analyses to the values used.

When the gas density and collisional quenching effects are low enough, diffusion of the excited molecules cannot be neglected and solutions to the appropriate rate equations must be obtained using the techniques of Reference 11. In this reference it was shown that to a good approximation we need consider only the fundamental diffusion mode as is done in Eqs. (1) and (2). Under these conditions it is convenient to express the results of Eq. (5) in terms of the steady-state magnitude, i.e.,

$$C^{\ddagger}(\infty) = \frac{W n_e n}{\nu_S} \frac{\alpha_C}{n} \tag{7}$$

where

$$\frac{\alpha_C}{n} = \frac{\nu_{XC}}{\nu_F} \frac{\alpha_{eX}}{n} + \frac{\nu_X}{\nu_F} \frac{\alpha_{eC}}{n} \quad . \tag{8}$$

Thus, α_C/n is an effective excitation coefficient for the production of $C^{\ddagger}$ molecules. We will compare values of α_C/n calculated using the Boltzmann equation and our cross section sets with our experimental results. Note that when excitation transfer between the homonuclear species X and the carbon containing species is C rapid enough $\nu_X = \nu_{XC}$, $\nu_F = \nu_{XC} + \nu_{CX}$, and

$$\frac{\alpha_C}{n} = \frac{\nu_{XC}}{\nu_F} \left(\frac{\alpha_X}{n} + \frac{\alpha_C}{n}\right) \quad . \tag{9}$$

This collisional equilibrium condition is a good approximation for our N_2-CO_2 and N_2-CO mixtures (References 10, 12-14), but not for the other mixtures considered here.

Most experimental studies of the kinetics of these vibrational states have been performed at high enough gas densities such that diffusion can be neglected and the results expressed as effective rate coefficients defined by

$$k_S = \frac{\nu_S}{n} \quad \text{and} \quad k_F = \frac{\nu_F}{n} \quad . \tag{10}$$

We will use plots of k_S and k_F versus the fractional CO or CO_2 density $X_C = [CO]/n$ or $[CO_2]/n$ to summarize the available kinetics data.

In other experiments (References 12-14) in which a pulsed laser is used to excite the carbon containing molecules, kinetics information is obtained from the ratio of the magnitudes of the two observed exponential components. In our notation the ratio R of the magnitude of the fast component to the magnitude of the slow component is given by

$$R = \frac{\nu_F - \nu_X}{\nu_X - \nu_S} \quad . \tag{11}$$

In the limits of $\nu_C > \nu_{CX}$ and $\nu_X > \nu_{XC}$ as at large X_C or of $\nu_{XC}\nu_{CX} \ll \nu_C\nu_X$ as at low X_C then

$$R = \frac{\nu_{CX}}{\nu_{XC}} \quad ,$$

i.e., R is determined primarily by the equilibrium concentration ratio between $X^\ddagger$ and $C^\ddagger$ and is very insensitive to the excitation transfer rate coefficient. This is the situation for most gases for which R has been observed.

The relation of the excited molecule density given by Eq. (5) and the observed signal is discussed in detail in References 10 and 11 and will not be repeated here. These authors show that the excitation coefficient for the production of vibrationally excited carbon containing molecules $C^{\ddagger}$ is given by Eq. (17) of Reference 10, i.e., by

$$\frac{\alpha_C}{n} = \frac{Cq\ \nu_S S_o}{GIAn\ S_r\ T} \quad , \tag{12}$$

where

$$C = \frac{4\pi\ f_r\ a\ R_b^2\ e}{R_d^2\ L} \int_0^\infty f_i(\lambda)\ B(\lambda) d\lambda \quad . \tag{13}$$

Here q is the ratio of the total drift tube current I to the electron component of the current as defined in Reference 11, ν_S is the slow decay obtained by fitting exponentials to the measured infrared emission signal, S is the steady-state or late-time value of the infrared signal, S_r is the signal measured when the detector is illuminated by blackbody reference source, G is the geometrical correction for spatial variations in the detector sensitivity and in the excited state density caused by the combined effects of excited molecule diffusion and of electron attachment and ionization, A and T are the radiative transition probability and fractional transmission for the observed infrared band. In Eq. (13) f_r and $f_i(\lambda)$ are the fractional tranmissions of the drift tube window at the reference and of the interference filter used to limit the infrared emission from the reference source, λ is the wavelength, a is the area of the aperture placed at

the blackbody to limit the reference signal, R_b and R_d are the distances from the detector to the aperture at the blackbody and to the center of the drift tube, L is the separation of the drift tube electrodes, $B(\lambda)$ is the blackbody emissivity per unit area, and e is the electronic charge. Note that since the interference filter is used only with the blackbody, the average of the filter transmission over the emission band which appears in Reference 11 is absent in Eq. (13).

An assumption made in the evaluation of ν_S from the observed infrared signals and in the calculation of G in Eq. (12) when diffusion is important is that only the slow exponential is important, i.e., that $\nu_F \gg \nu_S$. See Reference 11. This condition is satisfied satisfactorily for the gas mixtures examined, except for H_2-CO and for D_2-CO at low gas densities. These exceptions will be discussed further.

b. Infrared transmission

The transmission of the infrared emission from the vibrationally excited CO or CO_2 through the gas mixture is discussed in detail in Reference 10 and will not be repeated here. Figure 1 shows the results of our calculations of the fractional transmission for CO-N_2 and CO_2-N_2 mixtures. These calculations used the non-overlapping line approximation, transmission functions for isolated lines with Voigt profiles (Reference 16), and published line strength and broadening coefficients (References 17,18). As shown by the points in Fig. 1 from Reference 10, we find that at the higher gas densities used the transmission is a function only of the distance and the small fractional concentration

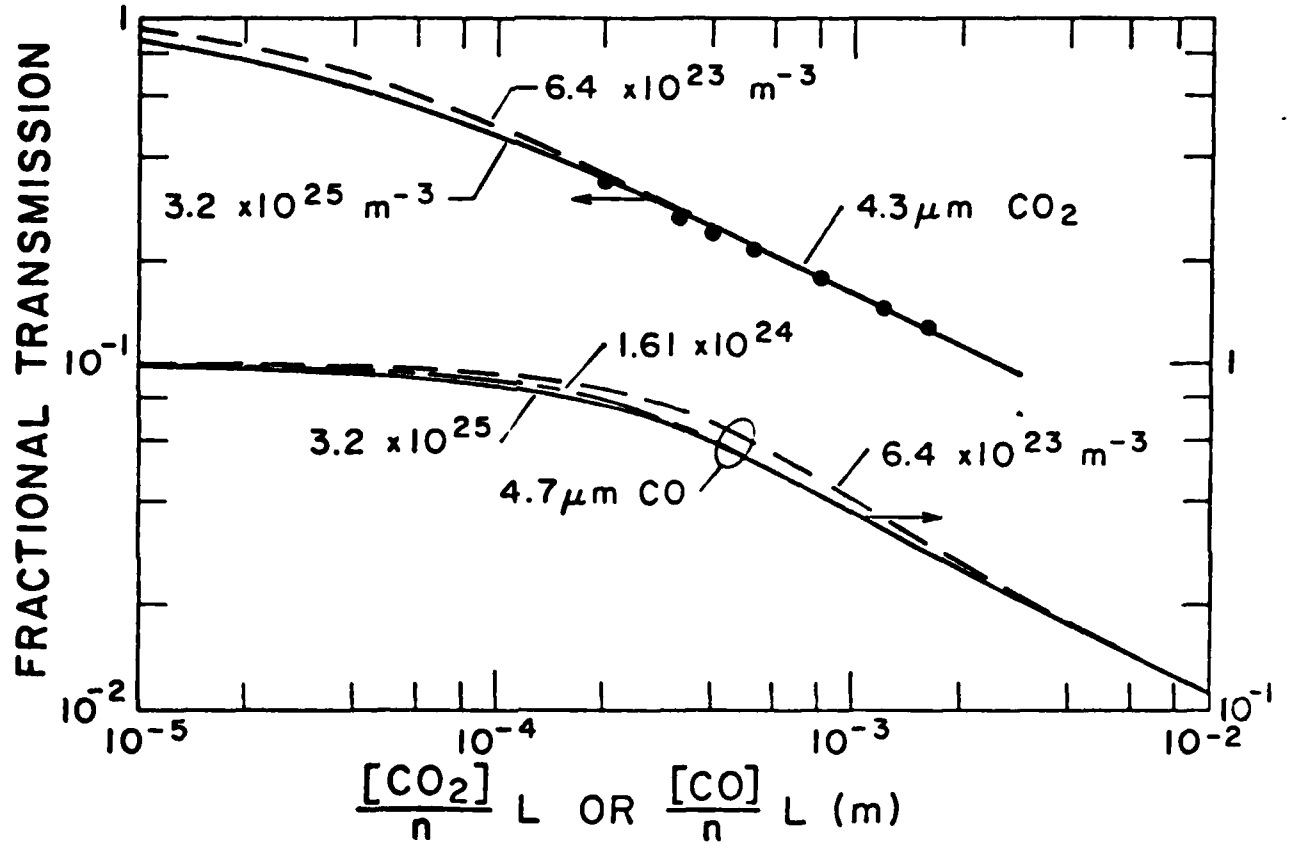

Figure 1. Calculated fractional transmission of the 4.3 μm band of CO_2 through N_2-CO_2 mixtures and of the 4.7 μm band of CO through N_2-CO mixtures. The solid lines are for the limit of high gas density, while the dashed lines show the effects of Doppler broadening at lower gas densities.

of the carbon containing molecule. This behavior is characteristic of collision broadened lines. At the lower gas densities Doppler broadening leads to an increased transmission. The coefficients for the broadening of the CO (Reference 19) and CO_2 (Reference 20) bands by D_2 and H_2 are as much as 20% different than those for N_2 and this was taken into account by scaling the curves of Fig. 1. It should be kept in mind that an assumption made in the derivation of Eq. (5) is that the loss of vibrationally excited molecules by radiation is small compared to the loss by collisional deexcitation so that any photon which is absorbed is lost. This is a good assumption except in D_2-CO mixtures, where we believe the resultant error in α_C/n is less than 5%.

c. Effect of ionization and attachment

At the higher E/n used in these experiments it is necessary to take into account the changes in electron density caused by electron impact ionization and attachment. Because of the low concentrations of the attaching gases, CO_2 and CO, used and because of the high rate coefficients for associative detachment of O^- with H_2, D_2 and CO (Reference 21), attachment contributions to q and G occur only for N_2-CO_2 mixtures and are made using theoretical attachment coefficients. Since ionization coefficients have not been measured in these gas mixtures, we have determined these coefficients both experimentally and theoretically. The experimental coefficients were found by analyzing the measured current versus E/n plots, such as shown in Fig. 2 for D_2-CO. The measured currents I at low E/n, e.g., below 4×10^{-20} V m^2 for the D_2-CO data, were fitted to theoretical values of the fraction of the cathode

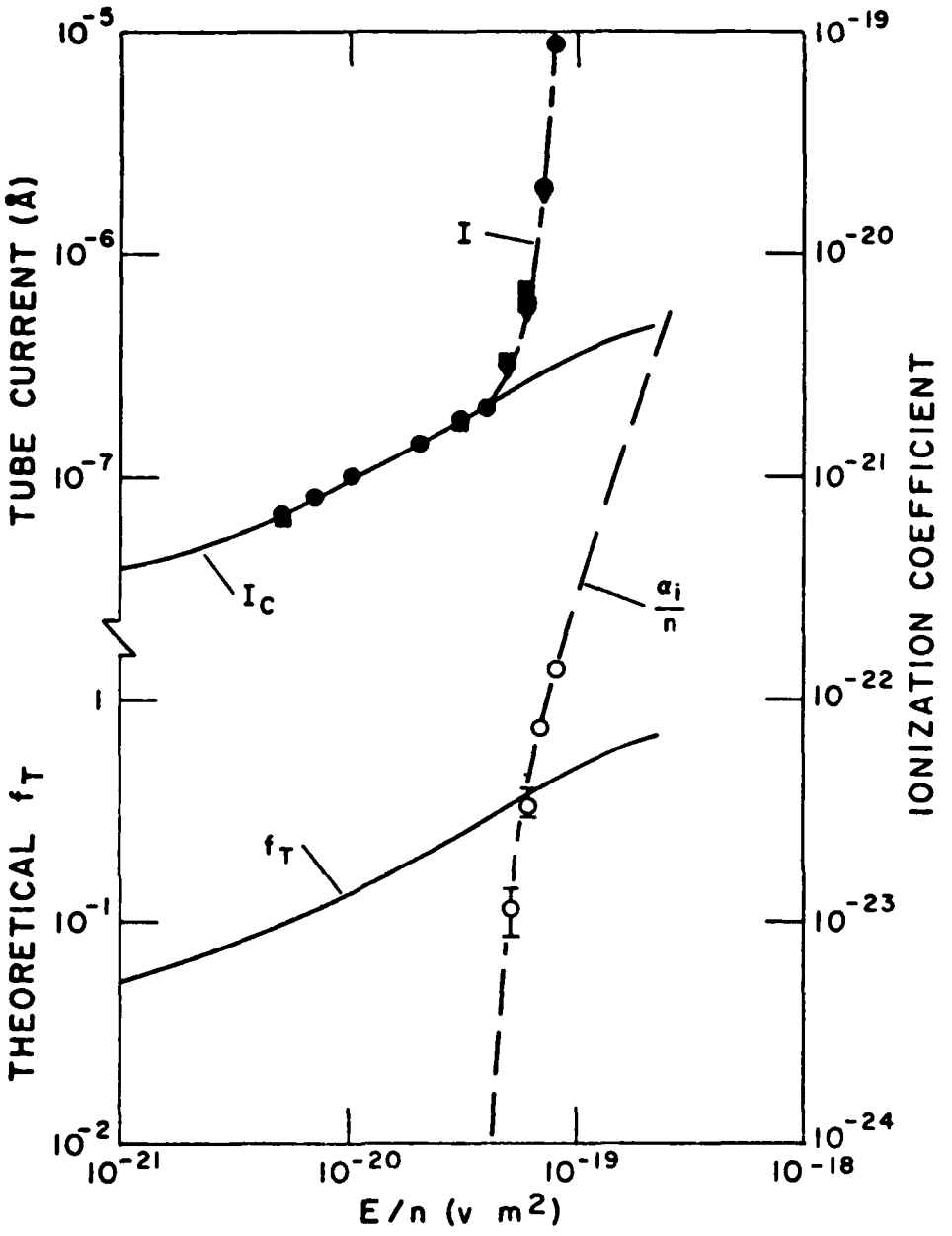

Figure 2. Current growth and ionization coefficient for a mixture of 0.998 H_2 and 0.002 CO. The lower solid line is fractional electron backscattering calculated using the Thompson theory, while the upper solid line is a fit of this theory to the measured currents. The solid points are the measured currents and the open points show ionization coefficients calculated from the measurements. The lower dashed curve shows calculated ionization coefficients and the upper dashed curve shows calculated currents normalized to the solid curve. Several sets of current measurements have been normalized at $E/n = 2 \times 10^{-20}$ V m^2. The total gas density was 6.44×10^{23} m^{-3}.

current crossing the drift tube as calculated using the Thompson formula (Reference 22) to yield curves of I_C versus E/n. This simple theory worked very well for the molecular gas mixtures of the present set of experiments. The ratio of the measured current to the extrapolated current I/I_C was then used in Eq. (13) of Reference 11 to obtain the ionization coefficient α_i/n, such as shown by the open points in Fig. 2. Ionization coefficients calculated using our final cross section sets for H_2 and D_2 (References 23, 24), such as shown by the dashed line in Fig. 2, agree well with the experimental values in the mixtures tested. Similar measurements and analyses of the variation of current with E/n at fixed gas density were carried out in pure N_2 and H_2 also yielded good agreement with conventional ionization coefficient determinations. The Penning ionization observed in collisions of excited D_2 with CO and CO_2 (Reference 25) was not detectable in our experiments. The theoretical curves of α_i/n were then used to calculate the q and G values for use in Eq. (12).

d. Theoretical excitation coefficients

The theoretical excitation coefficients for each vibrational level were calculated by solving the Boltzmann equation for the electron energy distribution and integrating over the vibrational cross section as in Reference 10. The excitation coefficients were then multiplied by the vibrational quantum number and added to obtain the total excitation coefficient for the v=1 level, i.e., the number of vibrational quanta was assumed to be preserved during the relaxation.

The vibrational temperature was low enough and the vibrational relaxation fast enough (References 26,27) so that the populations in levels with $v > 1$ could be neglected (Reference 12). In addition to direct vibrational excitation, we considered the results of electronic excitation with subsequent radiation to vibrationally excited levels using the branching ratios calculated by Hiskes (Reference 28). Even when we neglect V-T deexcitation of the higher vibrational levels (Reference 27) so that the number of $v = 1$ levels formed is equal to the original v value, we found that the maximum contribution of this excitation process was 10% at our highest E/n. Since gas phase recombination of H atoms (Reference 29) produced by electron excitation of the triplet levels of H_2 is improbable under our conditions and since wall recombination (Reference 2) would introduce long-time delays at most of our gas pressures, we believe that excitation and dissociation of the triplet states and subsequent formation of high vibrational levels of H_2 does not contribute significantly to our signals.

3. EXPERIMENT

The drift tube apparatus used in these experiments was the same as that described in Reference 11. The infrared blackbody source was the same as that of Reference 10, but the infrared detector was a special large area InSb detector operated at liquid N_2 temperature.

Most of the measurements were made at a gas density of 6.44×10^{23} m^{-3} (2660 Pa), although densities from 3 to 30 $\times$ 10^{23} m^{-3} were used. The mixtures were made by filling the system with the CO_2 or CO to a density of 6 to 60 $\times$ 10^{20} m^{-3} (5 to 50 Pa) and then adding the

O_2, H_2, or N_2. Gas pressures were measured with diaphram manometer with an estimated stated accuracy of ±0.5 Pa. This means that the mixture compositions were typically of ±10% accuracy, while the total density was accurate to about 1%.

A detailed discussion of the expected uncertainties in these measurements is given in Reference 11. However, for reasons which remain unknown the absolute intensity measurements appear to be in error by factors which were constant over a several month period, but which varied with the location of the interference filter used to select the portion of the blackbody spectrum reaching the detector. For this reason we have chosen to use the signal from the blackbody only as a day-to-day reference and to use the infrared emission from N_2-CO_2 and N_2-CO mixtures as the basis for normalization of the data from the mixtures of O_2 or H_2 with CO_2 or CO.

4. RESULTS

a. N_2-CO_2

The available collisional kinetics data for N_2-CO_2 mixtures has not changed significantly since it was summarized in Bulos and Phelps (Reference 10) and many other places (References 12,13,30). The rate coefficients which we used are listed in Table 1. The calculated values of ν_S are compared with our experimental values in Fig. 3. The agreement is very good. The calculated values of k_F are very large and vary only a few percent with the mixtures used. Since the calculated correction factors ν_F/ν_{XC} and ν_X/ν_{XC} appearing in Eq. (8) for our N_2-CO_2 mixtures are so close to the value expected for equilibrium

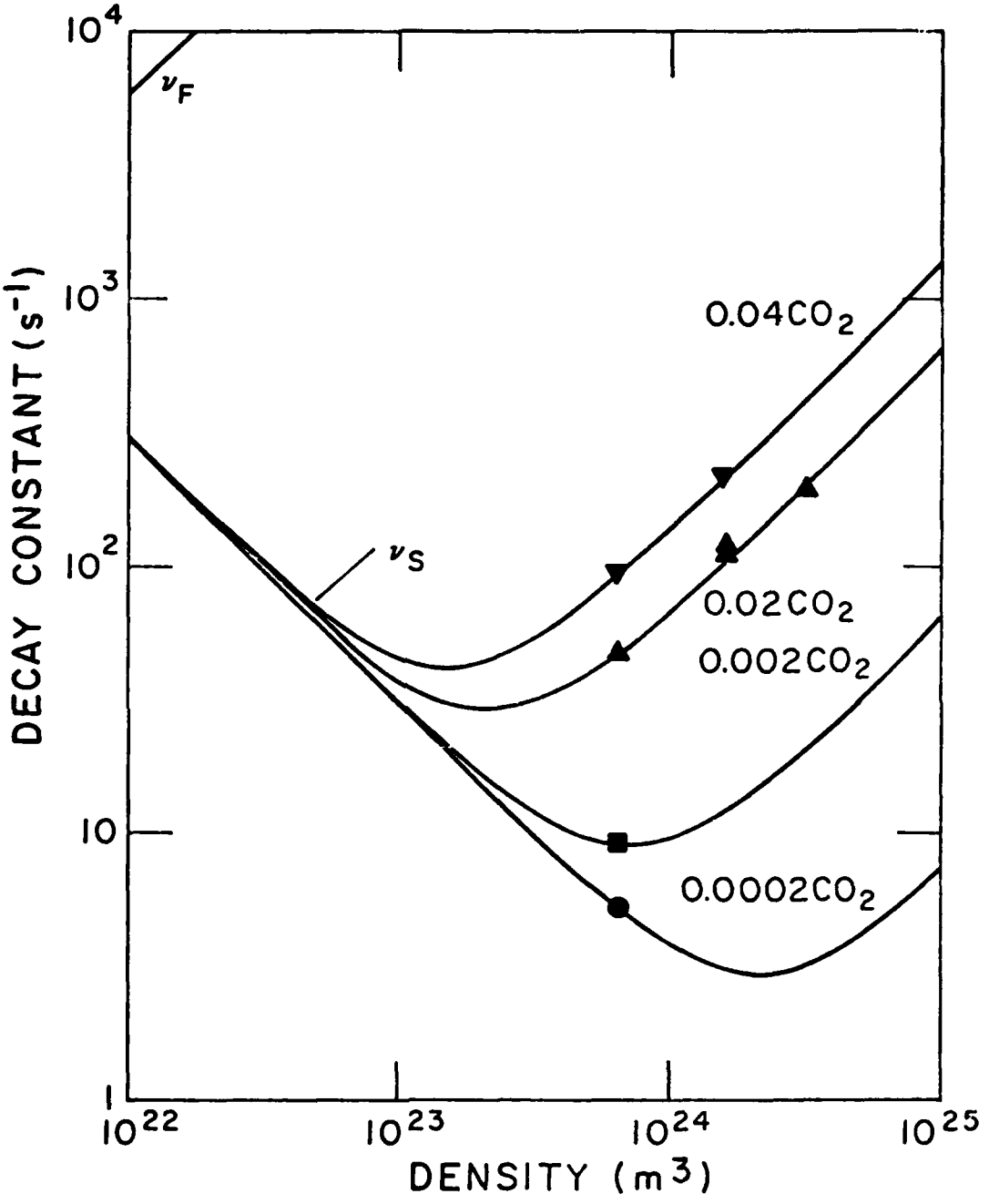

Figure 3. Decay constants for 4.3 μm emission from N_2-CO_2 mixtures. The curves are calculated using the rate coefficients listed in Table 1. The points are our experimental data.

between the excited N_2 and CO_2, we have not considered the kinetics of this system further.

To evaluate the contribution of ionization to q and G for N_2-CO_2 mixtures we used the attachment and ionization coefficients calculated using our current cross section sets for N_2 (Reference 31) and CO_2 (Reference 10).

The open points of Fig. 4 show the coefficients α_c/n for the excitation of CO_2 in a mixture of 0.98 N_2 and 0.02 CO_2 as calculated from our measured intensity of 4.3 μm radiation. Similar comparisons were made for mixtures containing 0.0002, 0.002, and 0.04 CO_2 in N_2. The average ratio of the experimental results to the predictions of solutions of the electron Boltzmann equation for these mixtures was 1.8±0.2. Since our previous measurements (Reference 10) for N_2-CO_2 mixtures gave agreement with theory to within 15% and since the efficiency of vibrational excitation of N_2 is 95±3% for $1 \times 10^{-20} < E/n < 5 \times 10^{-20}$ V m^2 (References 10, 32), we will reduce all of the 4.3 μm data by the factor of 1.8. Extensive efforts to determine the source of this discrepancy were unsuccessful. The solid points of Fig. 4 show the result of application of this factor to the data for 0.002 CO_2 in N_2. Note that the unnormalized data corresponds to an apparent energy efficiency of the system of at least 160%.

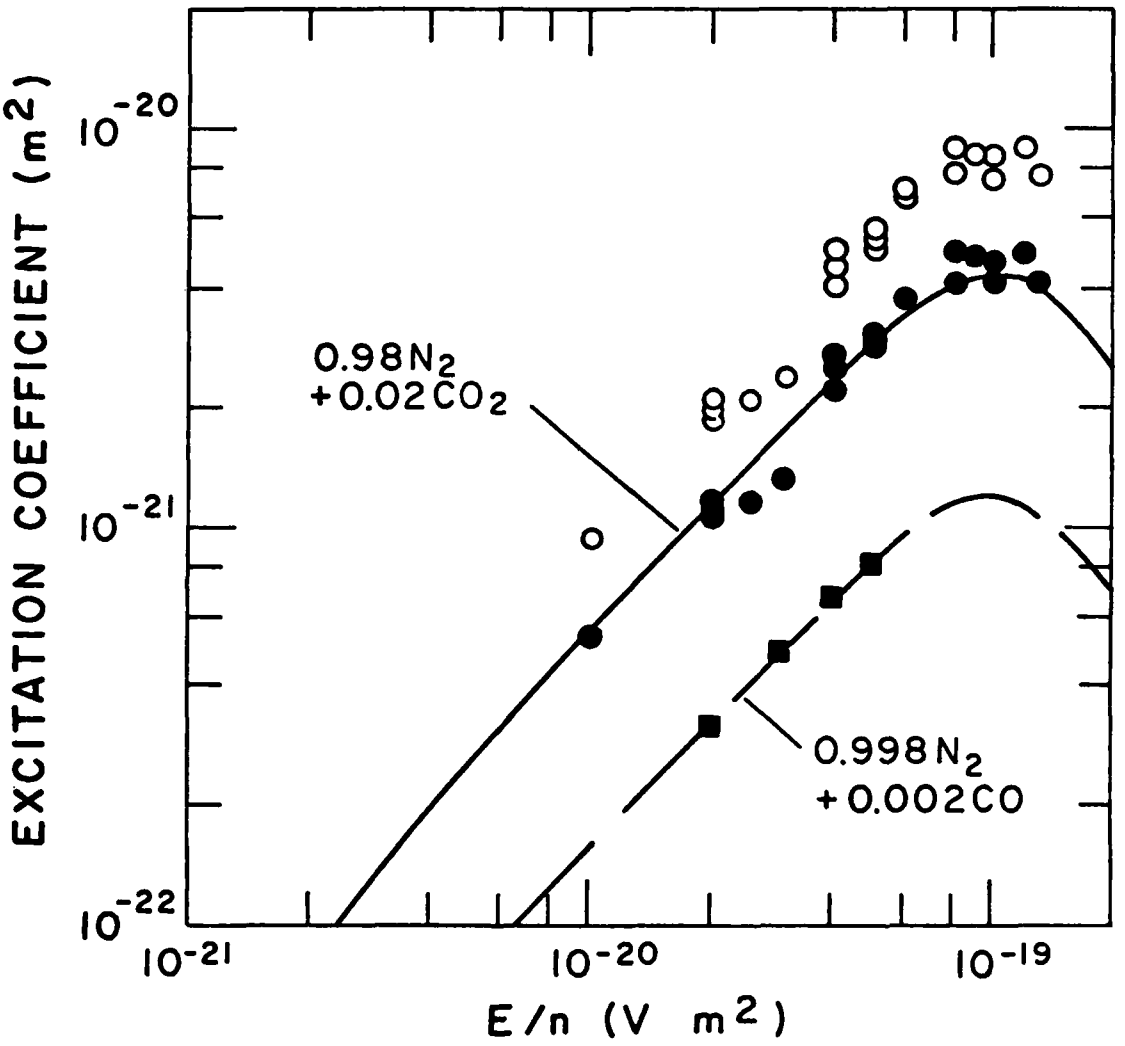

Figure 4. Effective excitation coefficients for production of vibrationally excited CO_2 and CO in mixtures with N_2. The open circles are our experimental results before normalization to our theoretical calculations. The solid points are normalized to our theory.

b. D_2-CO_2

The kinetics of the D_2-CO_2 system are most easily summarized by considering the plots of k_S and k_F in Fig. 5. The triangular points show the results of the measurements by Stephenson and Moore of the slow and fast decay constants for these gases (Reference 13). Also shown by the square points are the results of their measurements of the relative amplitudes of the fast and the slow components of the waveform observed when the CO_2 is excited with a short laser pulse. The lower rate coefficient for excitation transfer obtained more recently (Reference 33) is considered less reliable by its authors. Our measured values for the decay constants are corrected for diffusion (~10%) and are shown in Fig. 5 by the solid circles. Although measurements of self quenching of D_2 yield a wide range of values (References 34-37), our analysis is insensitive to this rate coefficient. Becuase of their self consistency and agreement with our measurements, we have adopted the rate coefficients of Stephenson and Moore. The solid curves show the results of the calculations using these rate coefficients as listed in Table I. The dashed curves show calculations of $k_X = k_{D_2}$ and $k_C = k_{CO_2}$ for D_2-CO_2 mixtures in the absence of diffusion. Note that for our D_2-CO_2 mixtures there are significant differences (40-60%) between the ν_{XC}/ν_F and ν_X/ν_F factors calculated using the rate coefficients of Table I and Fig. 5 and the values calculated assuming collisional equilibrium between the vibrationally excited D_2 and the 001 mode of CO_2.

Figure 6 shows a comparison of the effective excitation coefficient of Eq. (8) for 0.998 D_2 and 0.002 CO_2 from our experiments and

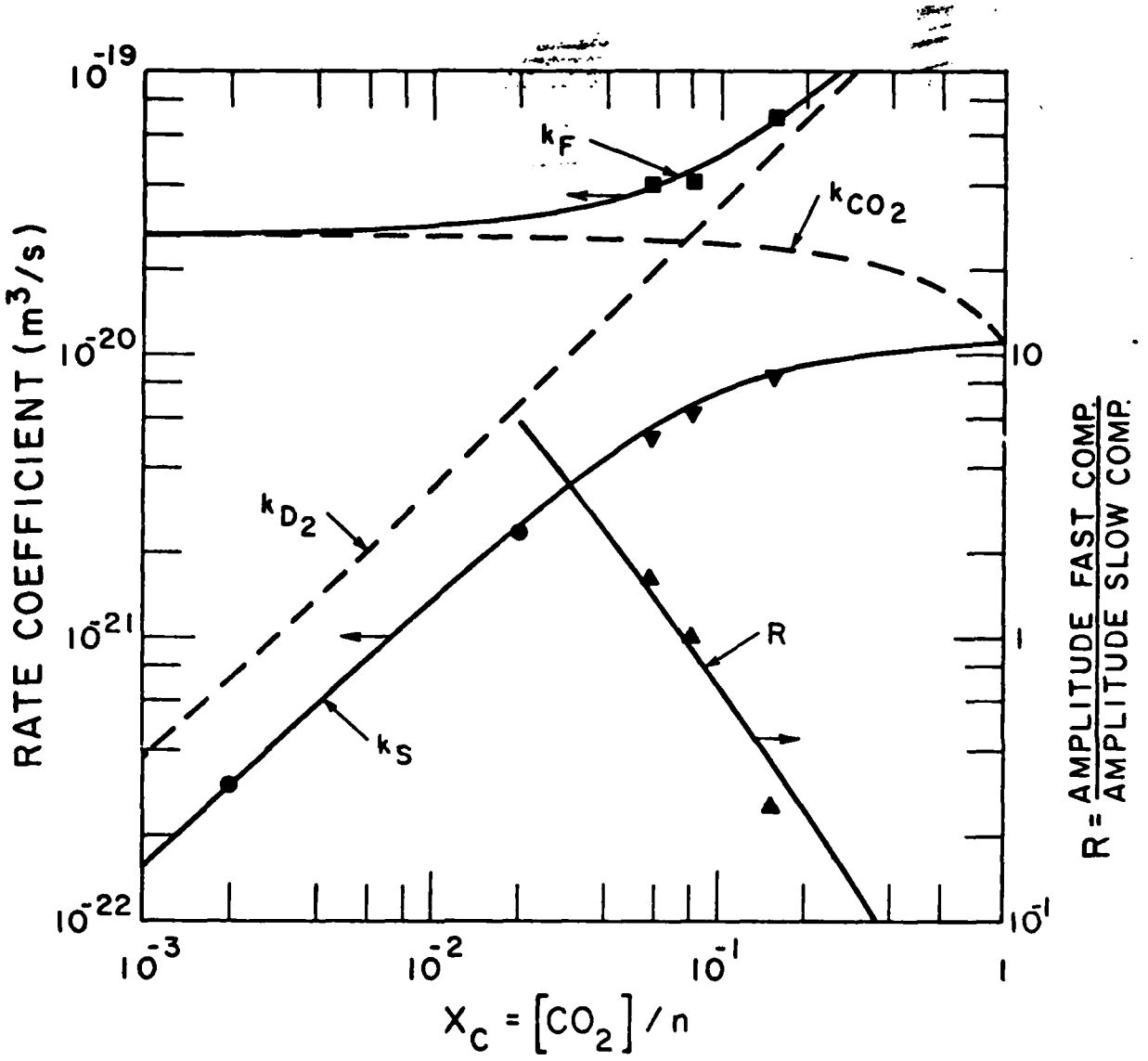

Figure 5. High pressure rate coefficients and relative amplitudes of emission components for D_2-CO_2 mixtures. Here k_F and k_S are the decay constants for fast and slow components of the emission, while R is the ratio of the amplitude of the fast to the slow component. The symbols and experimental references are: ● - our results after a small correction for diffusion; ■, ▼, ▲ - Reference 13.

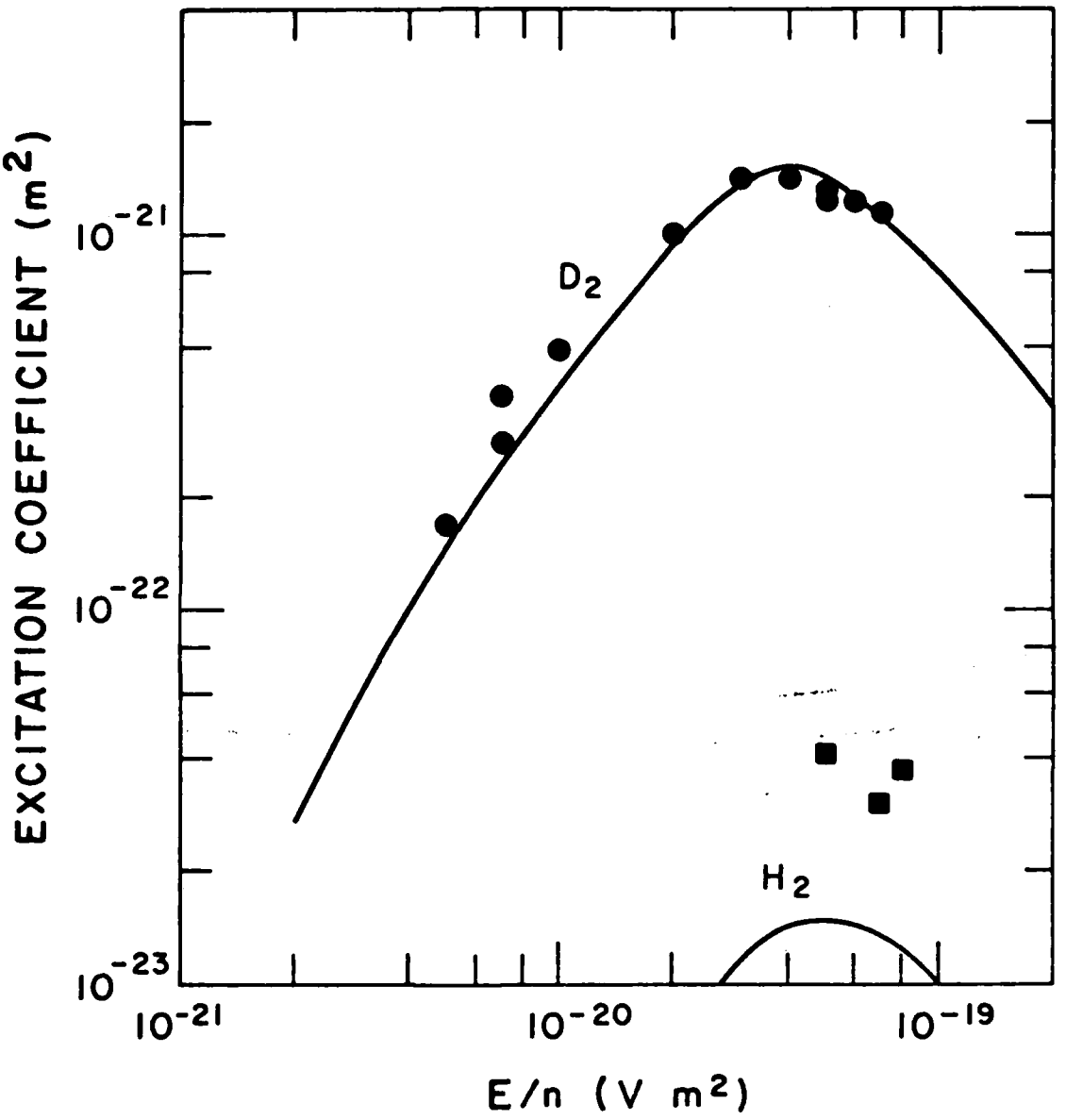

Figure 6. Effective excitation coefficient for the production of CO_2 in mixtures with D_2 and H_2. The points are our experimental data and the curves are from our theoretical calculations. $X_C = 0.002$.

from calculations using our current D_2 and CO_2 (Reference 10) cross section sets. For this mixture, the fraction of the excited CO_2 produced by direct excitation varied from 10% at low E/n to about 0.5% at high E/n. The average ratio of the experimental data for mixtures with 0.002 and 0.02 of CO_2 in D_2 is 0.98±0.16. It should be kept in mind that the experimental data for the D_2-CO_2 mixtures has been normalized using a scaling factor obtained by fitting the excitation coefficient data for N_2-CO_2 mixtures to theory as discussed in Section II2. One notes from Fig. 6 that the experimental excitation coefficient data very somewhat more slowly with E/n than does theory. This trend will be discussed further in connection with our D_2-CO results.

c. H_2-CO_2

The published high pressure rate coefficient data for H_2-CO_2 mixtures (References 33,38-43) are shown by the points in Fig. 7. The solid curves are calculated using the rate coefficients used in our analysis and given in Table 1. Our decay constant results are corrected for diffusion (~20%) and the average value is shown in Fig. 7 with an appropriate error bar. Because of the low concentration of CO_2 used, our signal is strongly dependent on the apparent rate coefficient for self quenching of H_2 (Reference 43), including the quenching of H_2 by impurities contained in the H_2. However, any such quenching is accounted for in our analysis through our measurement of ν_S and its application in Eq. (12). The more critical rate coefficient is that for excitation transfer k_{XC}^{VV}, since it determines ν_{XC} in Eq. (8). Our results seem to require a larger value than given in the

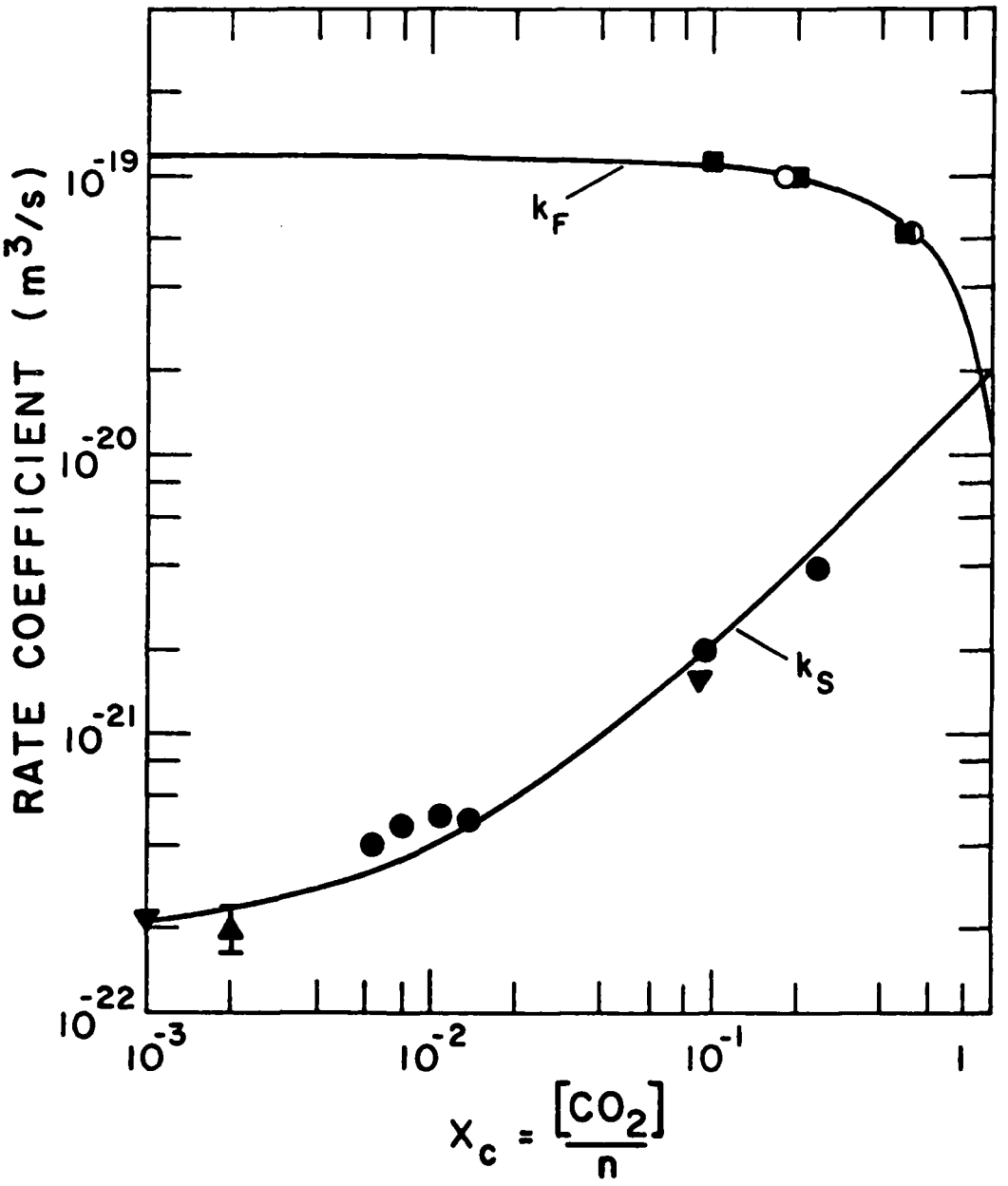

Figure 7. High pressure rate coefficients for H_2-CO_2 mixtures. The symbols and experimental references are: ▲ - our results after correction for diffusion; ○ - Reference 38; ■ - Reference 40; ▼ - Reference 41; ● - Reference 42.

literature (References 33,41,42). However, increasing it significantly beyond the value given in Table 1 and used to construct the curves in Fig. 7 would cause disagreement with the decay constant data.

The square points of Fig. 6 show the excitation coefficients calculated using Eq. (12) for a limited set of experiments with 0.002 CO_2 in H_2. The smooth curves show the excitation coefficients calculated using our current set of electron-H_2 (Reference 23) and electron-CO_2 (Reference 10) cross sections. Note that in spite of the low rate coefficient for excitation transfer from H_2 to CO_2, these calculations show that about 90% of the observed emission originates with electron excitation of the H_2. There is a discrepancy between theory and experiment of a factor of 2.7±0.4. A factor of two decrease in the discrepancy would occur if the vibrational excitation transfer were to the 002 level of CO_2 or to some nearby level with subsequent collision with CO_2 to form two molecules in the 001 level.

d. N_2-CO

The points of Fig. 8 show the experimental high pressure rate coefficients k_F and k_S observed in N_2-CO mixtures (References 14,44-48), while the solid curves show the values calculated using the rate coefficients listed in Table 1. The dashed curves labeled k_N and k_C show the decay constants characterizing the loss of vibrationally excited N_2 and CO, respectively, in the absence of significant population of the other excited level. One notes that there are very large discrepancies between the calculated curves for ν_S and the published experimental values. Our results are shown as an upper limit point because

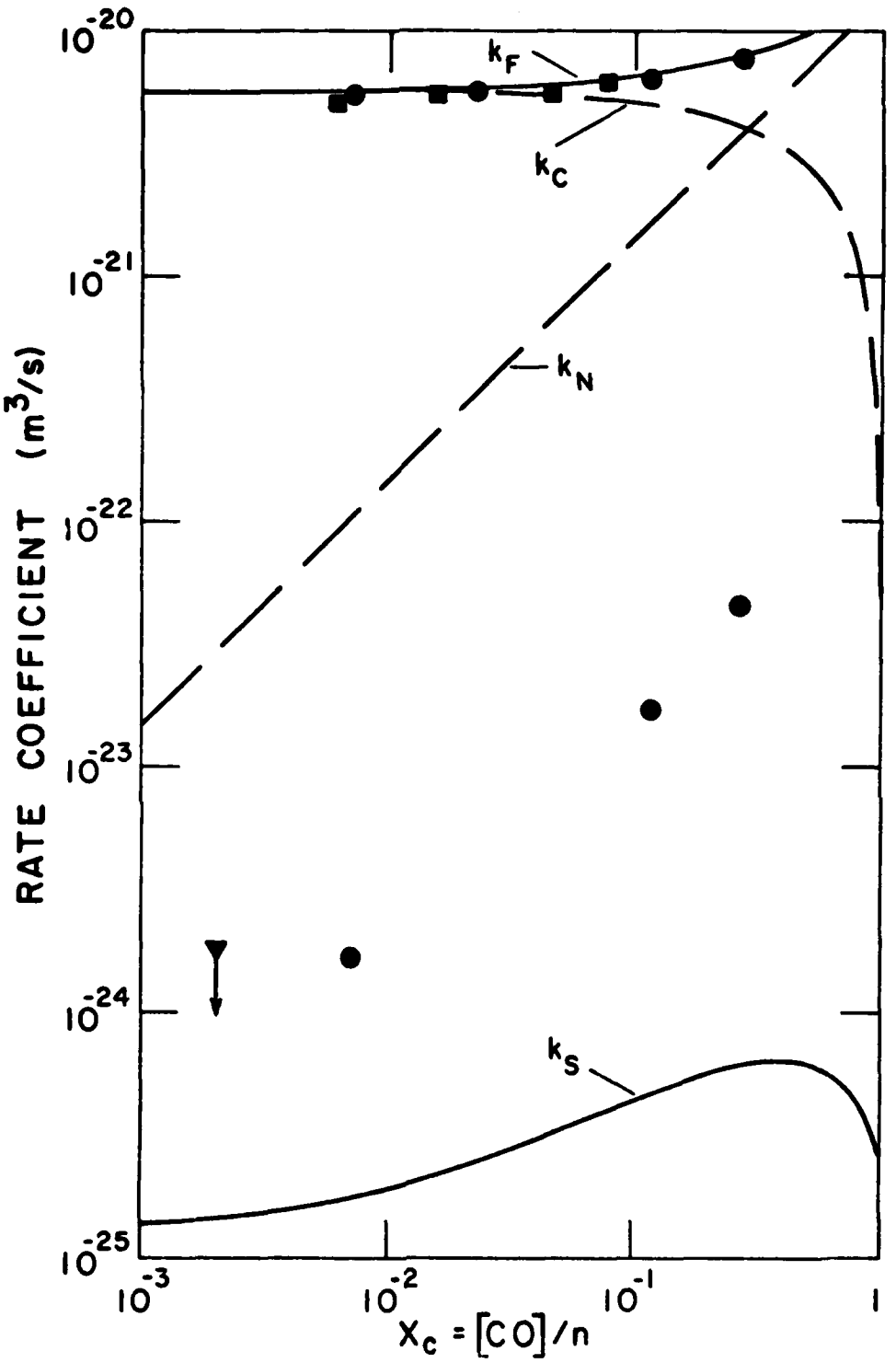

Figure 8. High pressure rate coefficients for N_2-CO mixtures. Symbols and experimental references are: ▼ - our results; ● - Reference 14; ■ - Reference 45.

of the very large and not accurately known correction for diffusion. Although cell dimensions are not given, it appears that the effects of radiation and diffusion loss should be small in most of the experimentms of Reference 14 so that the source of the excess quenching is unknown. Assuming that the "literature" values for the rate coefficients listed on Table I are approximately correct, we conclude that for the conditions of our experiment the populations of vibrationally excited N_2 and CO are in equilibrium at relative values determined by the gas temperature and the energy difference.

The dashed curve of Fig. 4 shows the excitation coefficients calculated using our current N_2 cross section set (Reference 31) and the CO cross section set from Land (Reference 49). Our experimental effective excitation coefficients are a factor of 2.54±0.07 larger than theory. We have no satisfactory explanation for this discrepancy. Since we believe that the theoretical α_C/n values are accurate to ±3% for $2 \times 10^{-20} < E/n < 5 \times 10^{-20}$ V m^2, we have applied a reduction of 2.54 to this and all other data obtained using CO emission. The solid squares of Fig. 4 show the resultant effective excitation coefficients for the 0.002 CO–0.998 N_2 mixture. In these experiments only 1 to 4% of the observed excitation is by electron excitation of the CO molecules.

e. D_2–CO

The present state of the kinetics of the D_2–CO system is represented by the experimental points (References 14, 36, 37, 50) shown in Fig. 9. The curves are calculated using the rate coefficients listed

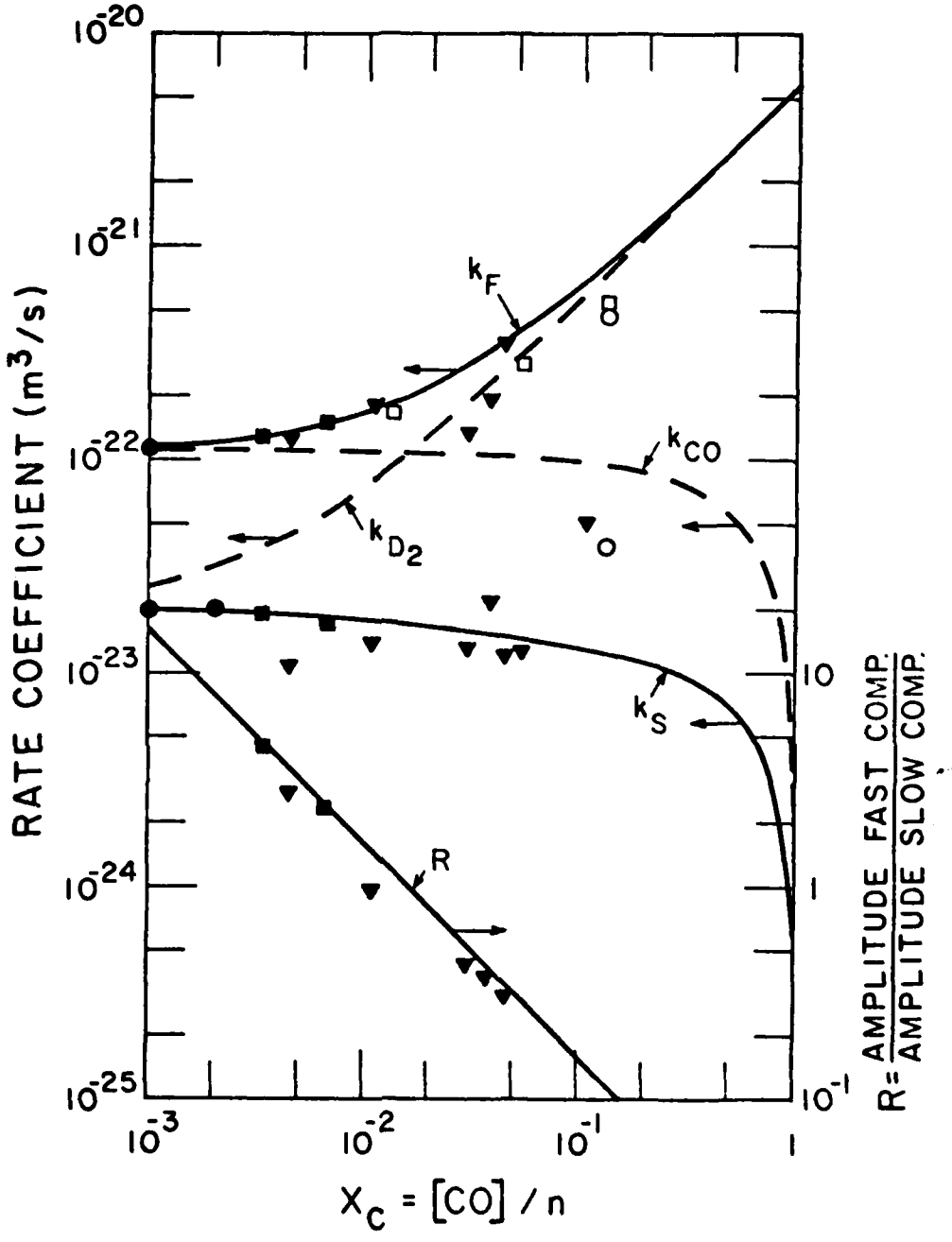

Figure 9. High pressure rate coefficients and ratio of magnitudes of fast and slow components of emission for mixtures of D_2 and CO. Symbols and references to experiment are: ● - our results after correction for diffusion; ■ - Reference 14; o - Reference 36; ▲ - Reference 37; ▼ - Reference 50.

in Table 1 and used in our analysis. Note that the calculations of the curves were carried out for a total density of 1×10^{26} m^{-3} in order to minimize diffusion and radiation contributions. These effects result in an increase in the apparent value of k_S by 20% for the lowest gas density used in Reference 50, i.e., the point near $X_C = 10^{-3}$ in Fig. 9. A disturbing feature of the experimental data is the rather large scatter and departures from the model at moderate fractional CO concentrations, since these are the data used to determine the value of the V-V excitation transfer rate coefficient k_{DC}^{VV}. This rate coefficient is much more important in the analyses of our experiments than is suggested by the near equilibrium population ratios because of the importance of diffusion in our experiments.

Our experimental decay constant data are corrected for diffusion and radiation and then plotted by the solid circles of Fig. 9. Note that we have included a value of ν_F calculated from a fit of the modification of Eq. (5) appropriate to a short excitation period (5 ms) followed by long (100 ms) decay. Unfortunately, our data were also obtained at such low CO concentrations that the decay constants are not sensitive to the excitation transfer rate coefficient.

It should be noted that at the highest E/n the drift tube current was about 10^{-5} A (see Fig. 2) and that the emission waveform showed significant deviations from the exponential behavior predicted by Eq. (5) and found at lower currents. We suspect that this behavior represents a loss of D_2 molecules in the v = 1 level as the result of collisions with other excited D_2, but have not carried the analysis

further. The data points to be shown for this E/n are obtained from fits to the initial rise in the infrared signal and so are relatively insensitive to this process.

The points of Fig. 10 show the vibrational excitation coefficients calculated using our experimentally measured intensities and our kinetics model for D_2-CO. The curves are calculated using our cross section sets for D_2 and CO. The average ratio of the experimental data shown in Fig. 10 to the calculated curves is 1.0±0.2. The calculated contribution of direct excitation to the vibrational levels of CO is 20% at E/n = 2×10^{-20} V m^2 and decreases at lower and higher E/n.

f. H_2-CO

The kinetics of the H_2-CO mixtures are the least satisfactory of any mixture considered here. This situation results from the fact that the energy difference between vibrationally excited H_2 and CO is so large that the coefficient for V-V excitation transfer from CO to H_2 is so small that the only way to observe the process is to first excite the H_2 and then observe the CO emission. The experiments of Matsui et al. (Reference 36) were carried out at high vibrational temperatures where a nonlinear analysis is required and rate coefficient extraction is difficult. The later experiments of Miller and Handcock (Reference 42) in H_2-CO mixtures are stated to be preliminary and are only partially reported. Finally, our mesaured decay constants for H_2-CO mixtures show much more scatter then with the other mixtures

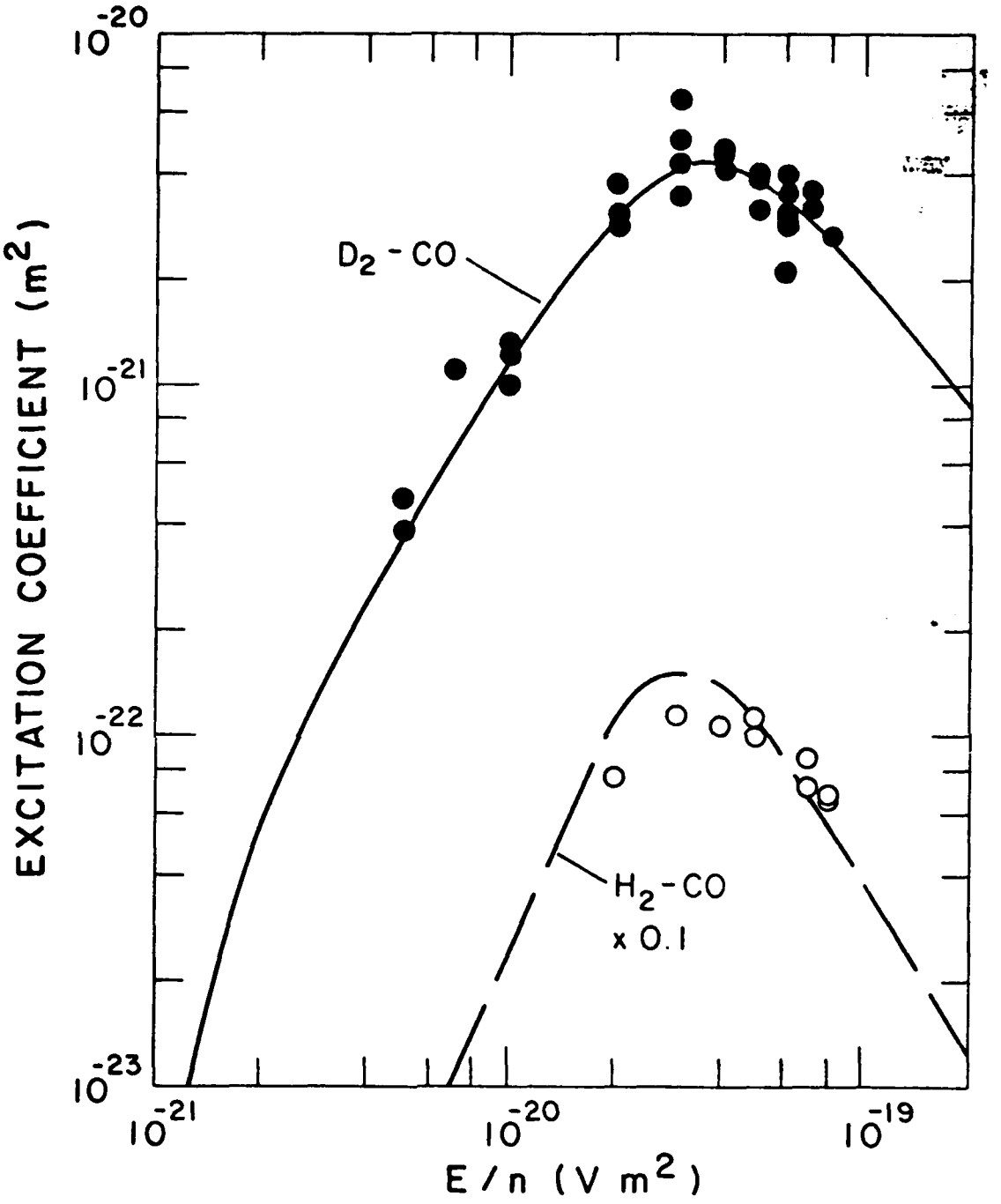

Figure 10. Effective excitation coefficient for the production of excited CO in mixtures of 0.002 CO and 0.998 D_2 or H_2. The points are our experimental results while the curves are calculated as described in the text.

because of the relatively low signals. The high pressure decay constant data expressed as rate coefficients for the fast and slow components of the decay are shown in Fig. 11. The various measurements of decay constants for the CO molecule (References 14,36,42,45,46), i.e., the "fast" component, are shown by the solid points and show little scatter. However, the measurements of the slow component of the decay as shown by the open points disagree badly. The weak or zero variation of the rate coefficient for the slow component with the CO concentration XC at the higher XC has been interpreted (Reference 36) as showing that the rate coefficient for V-V excitation transfer k_{XC}^{VV} from H_2 to CO is essentially equal to that for V-T quenching by the H_2 or by impurities in the H_2. The solid curves of Fig. 11 are calculated using rate coefficients given in Table 1. The dashed curve is calculated using the rate coefficients given by Reference 36. If the excitation transfer is from vibrationally excited H_2 to the closely resonant v=2 level of CO it is possible to increase the efficiency of 4.7 μm production via H_2 excitation by a factor of 2.

The open square point of Fig. 11 shows the average of our measured values for the slow decay constant after correction for diffusion by 2 to 10%. The large error bar reflects the large scatter in the decay constants. Because of the poor signal-to-noise ratio, we have not attempted to fit our data with the double exponential which one expects when excitation transfer occurs and when the values of k_S and k_F differ by only the factor of two shown in Fig. 11. The large and variable decay constants found in our experiments may be caused by the presence of impurities, such as carbonyls, since liquid N_2 was not

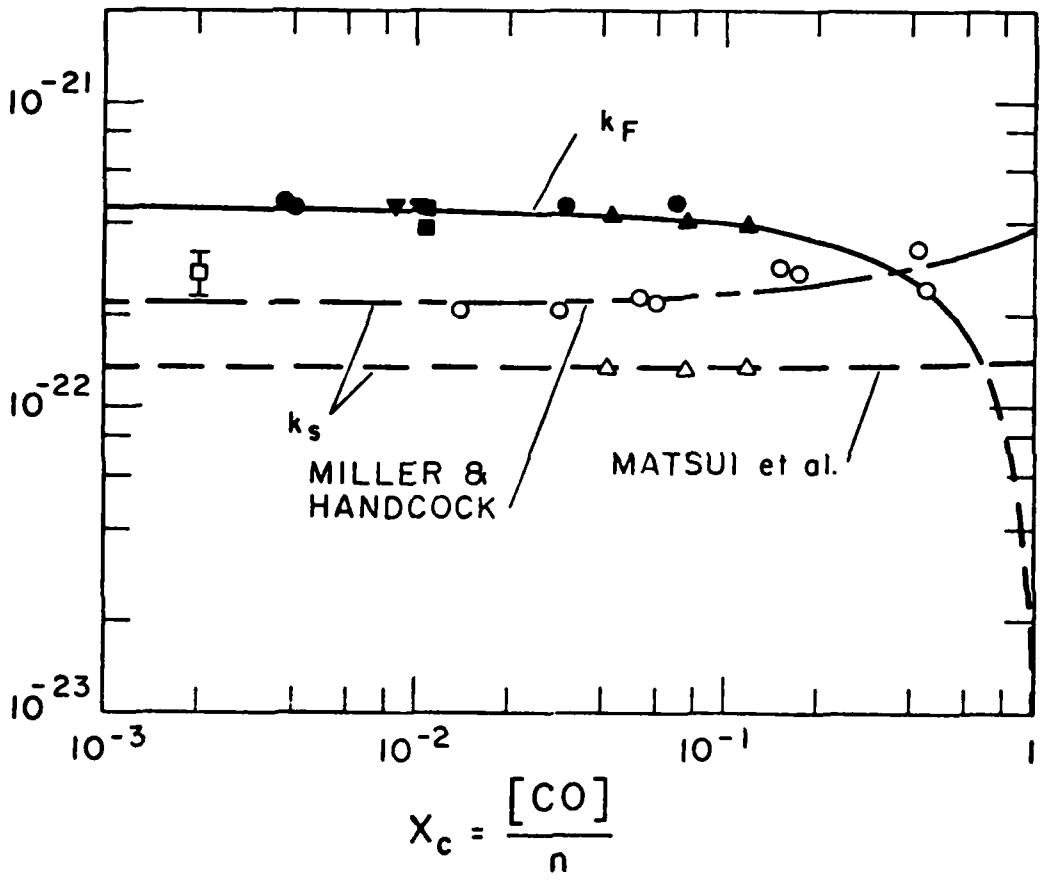

Figure 11. High pressure rate coefficients for mixtures of H_2 and CO. Symbols and references to experiment are: □ - our results after correction for diffusion; ● - Reference 14; ▲, Reference 36; ○ Reference 42; ▼ - Reference 45; ■ - Reference 46.

used with the H_2-CO mixtures. It should be recalled that to a good approximation the effects of such impurities on the excitation rate coefficients are accounted for through our measurement and use of ν_s in Eq. (12).

The vibrational excitation coefficients calculated from our measured intensities of 4.7 μm emission are shown by the points of Fig. 10. The curve shows the theoretical prediction calculated using our cross section sets. The calculations show that more than 90% of the observed signal originates with electron excitation of the CO, i.e., there is very little excitation transfer from the H_2 to the CO. The average value of the ratio of the experimental to theoretical excitation coefficients is 0.9±0.2. Such a small discrepancy may seem surprising in view of the uncertainty in the rate coefficients. However, this result is consistent with the relative lack of importance of excitation transfer compared to direct excitation. The small contribution of excitation transfer to the production and destruction of vibrationally excited CO explains the absence of a second exponential in our data.

5. DISCUSSION

The experimental results presented in Section II.4 demonstrate that one can measure the coefficients for electron excitation of the vibrational levels of molecules such as D_2 by electrons using the tracer technique. The comparisons of experimental results with theoretically calculated excitation coefficients shows generally good agreement when the signal-to-noise ratios are good and where the rate coefficients for the vibrational levels are well known. This is seen

in the comparison of experimental and theoretical total excitation coefficients versus E/n for D_2-CO_2 mixtures shown in Fig. 12. Such a plot is meaningful for a nonequilibrium case such as D_2-CO, as well as mixtures where equilibrium applies such as N_2-CO_2 and N_2-CO, because of the near equality of ν_X and ν_{XC} in Eq. (8), i.e., the small rate of quenching of D_2 compared to that for excitation transfer to CO_2 for our experimental conditions. This plot has the advantage of allowing a comparison of data obtained at different fractional concentrations of the carbon containing molecule, e.g., 0.02 and 0.002 CO_2 in D_2. In this case the scatter in the data is larger than the predicted differences for the two mixtures. The experimental excitation coefficient data show a systematic tendency to vary more slowly with E/n or electron energy than do the calculated coefficients. The mean electron energies for the experimental data of Fig. 12 increases from 0.45 to 4.5 eV as the E/n is increased from 5 to 80 $\times$ 10^{-21} V m^2. As pointed out in Section III, the contribution of cascading following excitation of the singlet states is 10% or less at our highest E/n and so does not explain this tendency.

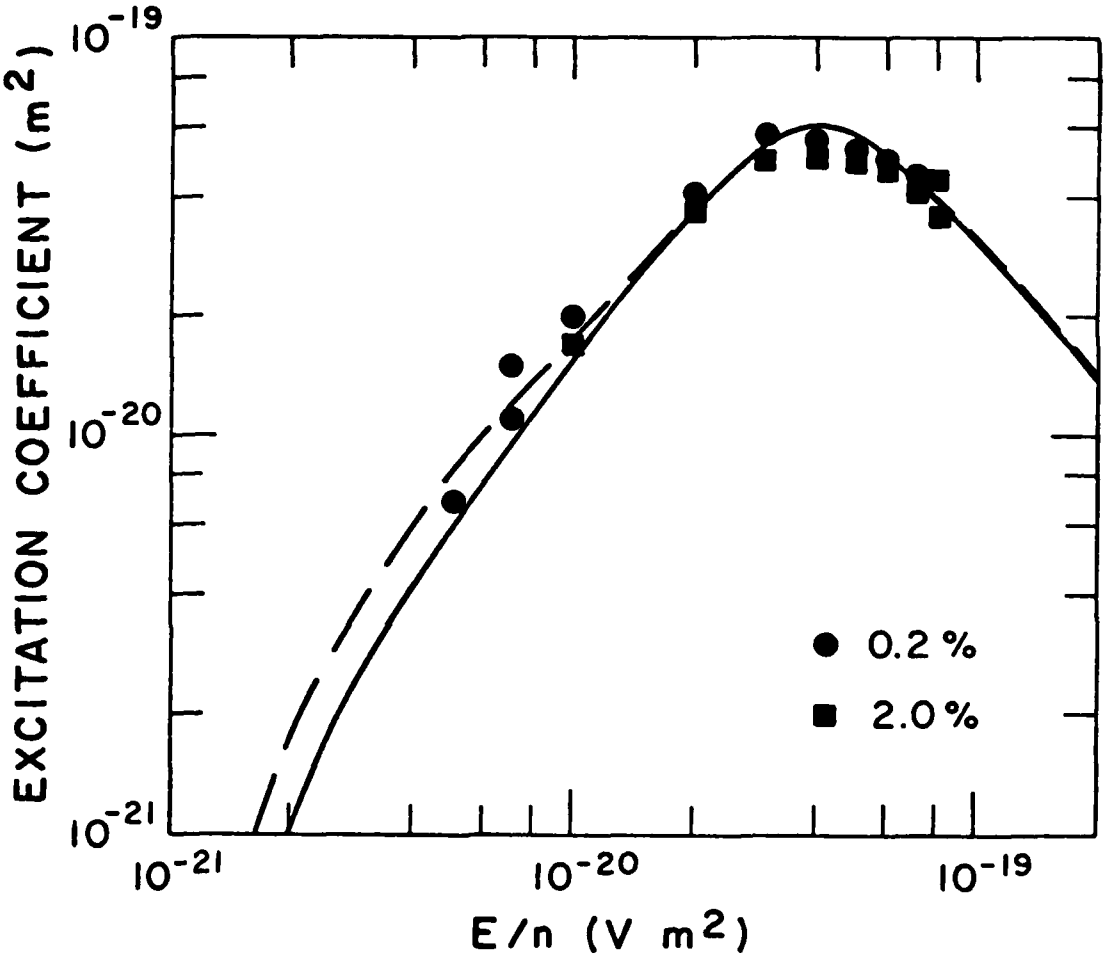

Figure 12. Total vibrational excitation coefficients in D_2-CO mixtures. The symbols are: ● - 0.002 CO; ■ - 0.02 CO. The dashed and solid curves are calculated for 0.02 and 0.002 CO in D_2.

SECTION III

DETECTION OF EXCITED STATES BY LASER-INDUCED FLUORESCENCE

The objectives of this research are: a) the development and application of laser fluorescence techniques to measurement of excited state densities in electric discharges, b) to develop and apply other diagnostic techniques, such as absolute emission intensities, to the determination of the characteristics of moderate current density electrical discharges, and c) the quantitative comparison of these results with appropriate discharge models. These objectives are part of our overall program to develop the diagnostics and models required for measurement and prediction of the properties of electrical discharges in molecular gases. Such discharges are of interest to the Air Force because of their utility in devices such as high power switches, negative ion sources and radio frequency discharge processing and because of their role in phenomena such as lightening and corona.

Because of recent interest in the use of H_2 in negative ion sources and thyratron switches and because of the lack of data on the electron excitation and collisional destruction of excited H_2, we have chosen to develop and apply these techniques to the $a^3\Sigma_g^+$ and $c^3\Pi_u$ states of H_2. Figure 13 shows the energy levels of H_2 of interest in the present experiments. Also shown are one of the possible laser absorption transitions and the uv emission transitions from the $a^3\Pi$ and laser excited state. The $a^3\Sigma_g^+$ state is the upper state of the near uv continuum of H_2 and has a sufficient density in pulsed discharges to

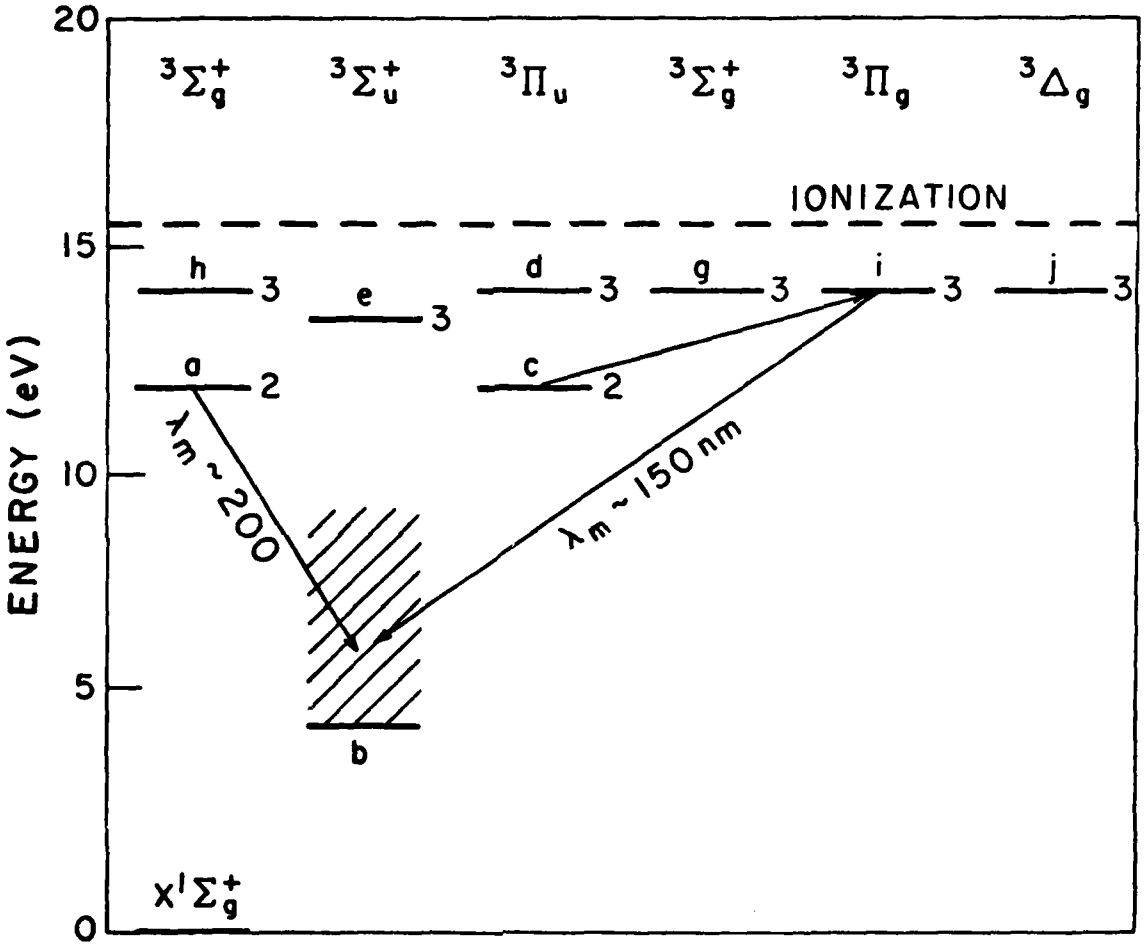

Figure 13. Energy level diagram for the lower states of the triplet system of H_2. The diagonal lines indicate the radiative transitions of interest in our experiments.

have been detected by absorption techniques (References 51-53). However, there is considerable disagreement as to the radiative lifetime and collisional kinetics for this state (References 54-59). The lowest vibrational level of the $c^3\Pi_u$ state of H_2 is metastable against radiation (Reference 60), but half of the rotational levels undergo rapid predissociation (Reference 61). Because of the small energy separation between the lowest vibrational levels of the $a^3\Pi$ and $c^3\Sigma$ states (194 cm^{-1}), there is the unconfirmed possibility of excitation transfer between these states (Reference 57).

1. EXCITATION OF NEAR UV CONTINUUM OF H_2

These measurements provide data on the collisional properties of H_2 molecules excited to the $a^3\Sigma_g^+$ state. In addition, they tested the operation of the drift tube at the much higher currents that would have to be used in any measurements of the density of the $c^3\Pi_u$ metastable state of H_2. There have been reports (Reference 57) of excitation transfer between the $a^3\Sigma$ state and some nearby state with a very short radiative lifetime. We have therefore carried out the steady-state version of such an experiment using our drift tube filled with pure H_2. The rate equations describing this experiment are the same as those of Section II2 with appropriate changes in notation. Although rapid energy transfer to the singlet states of H_2 may have occurred at the high gas temperatures of Reference 57, it seems very unlikely at our gas temperature of 300 K. We therefore assume that the collisional coupling is to the $c^3\Pi$ state. If the destruction of the $c^3\Pi$ state is by collisions, rather than by radiation or diffusion,

as we expect at the high H_2 densities of these experiments, then Eqs. (7) and (8) can be written as (Reference 62)

$$\frac{n}{[a]_\infty} = B\left[1 + \frac{k_{eff}\, n}{A_a}\right] \tag{14}$$

where

$$k_{eff} = k_a^{ET} + \frac{k_{ac}^{EE}\, k_c^{ET}}{k_c^{ET} + k_{ca}^{EE}} \quad . \tag{15}$$

Here $[a]_\infty$ is the steady-state concentration of H_2 $a^3\Sigma$ molecules and is proportional to the observed near uv emission, B is an unimportant constant determined from a fit of a straight line to Eq. (14), A_a is the radiative lifetime of the $a^3\Sigma$ state, k_{eff} is an effective quenching rate coefficient for the $a^3\Sigma$ state, k_a^{ET} and k_c^{ET} are the rate coefficients for collisional deexcitation of the a and c states by an electronic to translation ET or dissociation process, and k_{ca}^{EE} and k_{ac}^{EE} are the rate coefficients for excitation transfer from the metastable c state to the a state and from the a state to the metastable c state, respectively. In this formulation we have included the transfer of excitation to the $c^3\Pi$ states followed by immediate predissociation in k_a^{ET}. Figure 14 shows Eq. (14) fitted to our values of the ratio of the H_2 density to the signal after normalization to the tube current and after correction for ionization and spatial distribution, i.e., the q and G corrections of Section II. Data are shown for two different wavelengths in the near uv continuum. The effective rate coefficient for quenching of the $a^3\Sigma_g^+$ state derived from these data using the results of recent radiative lifetime measurements (Reference 54) is $(8\pm1) \times 10^{-16}$ m^3/s. From the

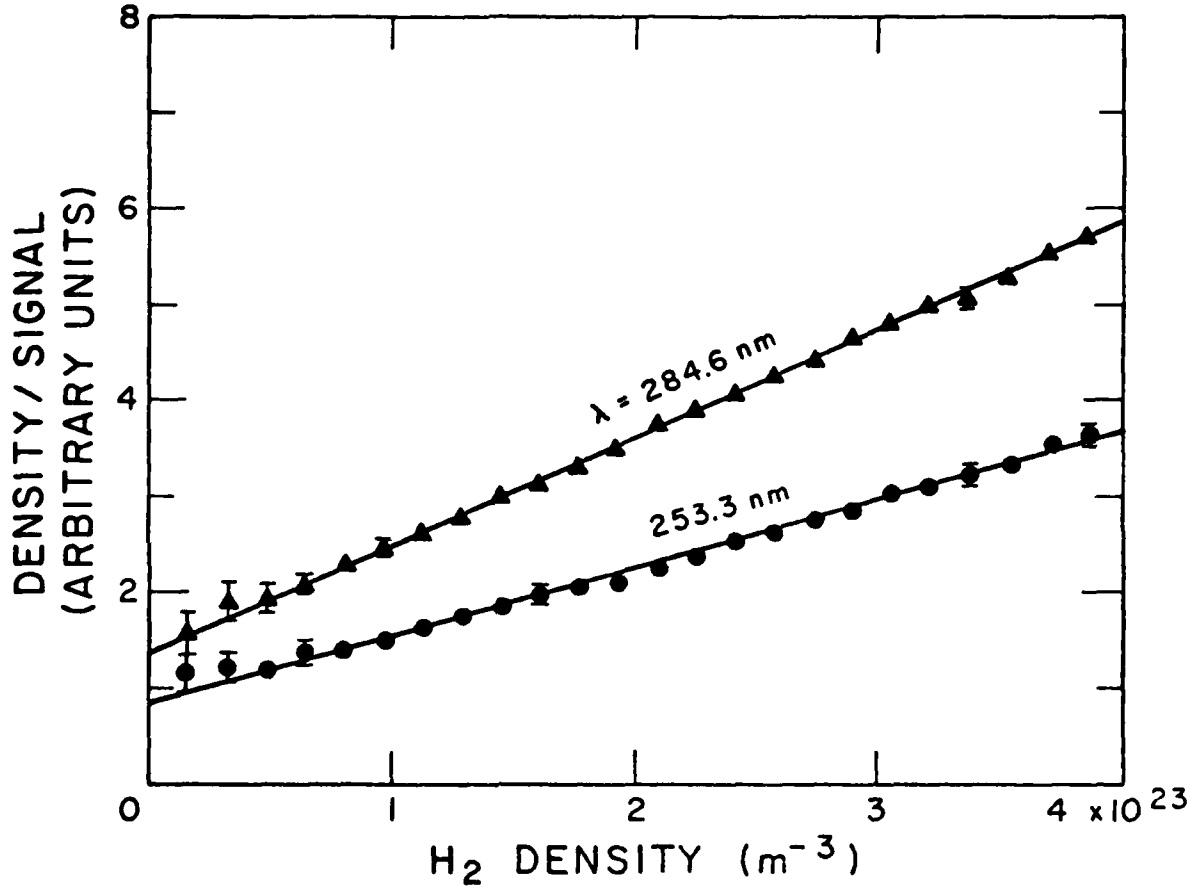

Figure 14. Variation of ratio of gas density to normalized near uv emission signal versus gas density for determination of quenching rate coefficient for the $a^3\Sigma_g^+$ state of H_2. The upper set of data is for the continuum near 284 nm while the lower set is for the continuum near 253 nm. The error bars are representative of the statistical uncertainty in the number of counts recorded.

absence of departures from the straight lines we conclude that at these H_2 densities any $a^3\Sigma$ molecules which undergo excitation transfer to the $c^3\Pi_u$ state are not destroyed by radiation or diffusion before returning to the $a^3\Sigma$ state. The published data on quenching of the $a^3\Sigma$ state are summarized in Table 2. Unfortunately, the absence of departures from a straight line means that we are unable to evaluate the rate coefficients for collisional coupling of the a and c states, i.e., k_{ac}^{EE} and k_{ca}^{EE}. Our effective quenching rate coefficient is significanly larger than that of Center (Reference 56) even when Center's data are reanalyzed using the radiative lifetime of Reference 54. We have not attempted to reanalyze the data of References 57 and 59.

2. LASER FLUORESCENCE EXPERIMENT

The objectives of this work are to develop and apply laser techniques to the measurement of the densities of excited molecules, such as H_2 metastables, in electrical discharges and to determine the rates of critical process controlling the excited state densities. In particular, we are investigating the applicability of laser fluorescence techniques to the measurement of the densities and collisional kinetics of the $c^3\Pi_u$ metastable state of H_2. A very much simplified term level diagram showing some of the excited states of H_2 relevant to our laser fluorescence experiment is shown in Fig. 15. An approximate description of the principle processes occurring in our low current discharge is as follows: At room temperature most of the H_2 molecules are in the orthohydrogen form and most of these molecules have a rotational quantum number of N = 1. For this discussion we assume that they are

Table 2. Quenching of $H_2(a^3\Sigma_g^+)$

Authors	T_g K	$n \times 10^{-22}$ m^{-3}	k_{eff}/A_a m^3	k_{eft} m^3/s	Ref.
Beare and Von Engel	293	80-300	5.2×10^{-25}	$\sim 4.6 \times 10^{-17}$	55
Center	300	4-60	5.3×10^{-24}	5.5×10^{-16}	56
Thompson and Fowler	1200	0.06-120	---	1.8×10^{-16}	57
Godart and Puech	293	*	---	1.8×10^{-16}	59
This work	300	1.5-50	8.2×10^{-24}	8×10^{-16}	

*H_2-Ar mixtures.

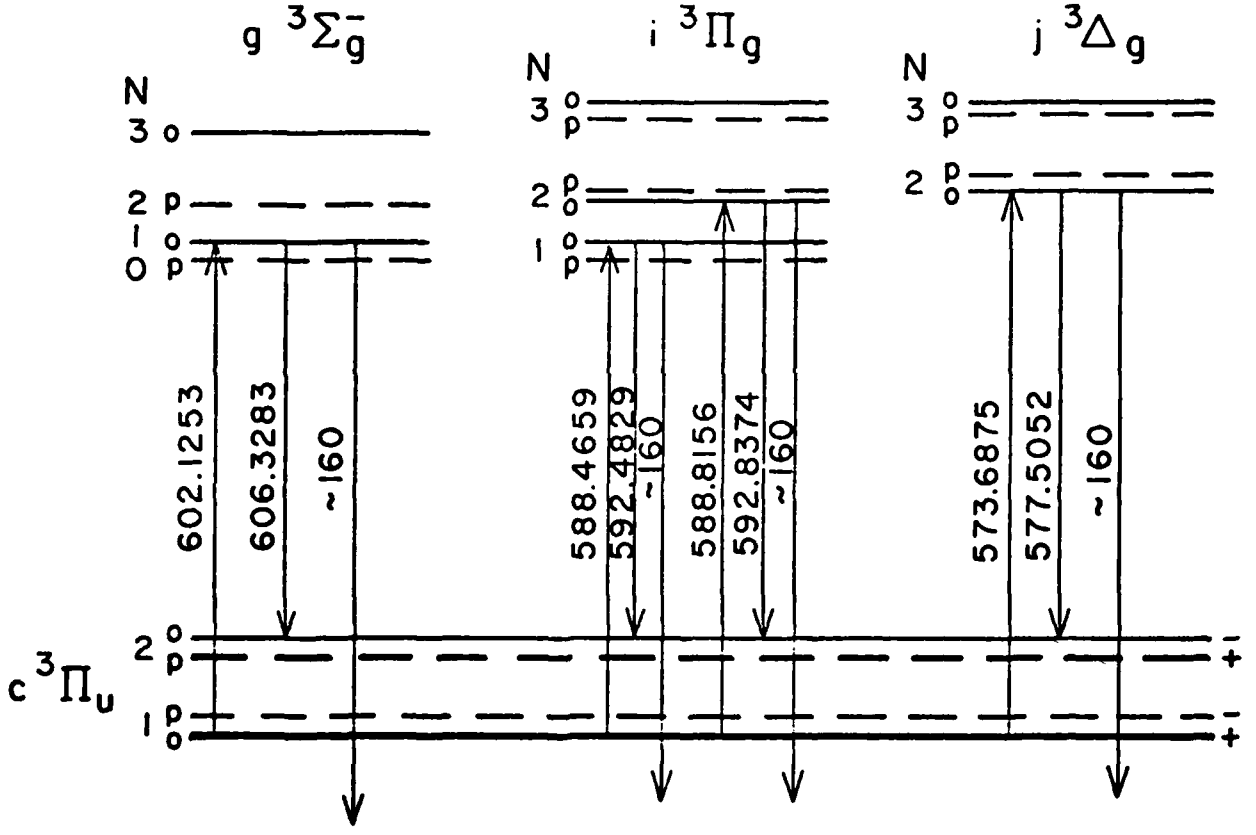

Figure 15. Simplified energy level diagram showing excited states and radiative transitions of interest in our search for laser-induced fluorescence from the $c^4\Pi_u$ metastable state of H_2. The wavelengths are in nm.

in the lowest vibrational level v = 0 of the ground electronic state $X^1\Sigma_g^+$. The H_2 $c^3\Pi_u$ metastable molecules of interest are assumed to be produced by electron impact excitation without change in the rotational quantum number, i.e., in the N = 1 level, and with 10 to 20% in each of the lower vibrational levels, v = 0 to 5. Note that the effects of known resonances in the excitation cross section near threshold could allow a change in the rotational quantum number. Molecules produced in the $c^3\Pi_u^-$ states, e.g., the N = 1 level of parahydrogen and the N = 2 level of orthohydrogen, undergo predissociation in about 3×10^{-9} s, while molecules in the $c^3\Pi_u^+$ state, e.g., the N = 1 and 3 levels of orthohydrogen, have radiative lifetimes of 0.1 to 1 ms depending on the vibrational level (Reference 60). Present predictions of theory (Reference 63) are that the molecules in the $c^3\Pi_u^+$ metastable levels will be rotationally excited to $c^3\Pi_u^-$ levels at an appreciable fraction of the gas kinetic rate coefficient and will immediately undergo predissociation. Assuming that the metastables will be destroyed by rotational excitation to the $c^3\Pi_u^-$ state with a rate coefficient of roughly 10^{-16} m^3/s or will diffuse to the electrodes in times of the order of 10^{-6} s, the metastable lifetime in our apparatus will be less than 10^{-5} s. This means that few of the $a^3\Sigma$ molecules are expected to live long enough to radiate, i.e., all vibrational levels of the $c^3\Pi_u^+$ state with N = 1 should be regarded as "metastable." We therefore expect the maximum $c^3\Pi$ lifetime to occur at H_2 densities of roughly 10^{21} m^{-3} and the metastable densities per unit current to be independent of density at higher H_2 densities.

Figure 15 shows some of the wavelengths we have selected from the literature (Reference 64) as most likely to show measurable

fluorescence. The upward or absorption transitions have been induced by tunable dye lasers and detected by visible fluorescence (Reference 65), metastable beam depletion (Reference 66), optogalvanic techniques (Reference 67) and uv fluorescence (Reference 68).

To increase the excited state densities over those available with the drift tube we have constructed narrow bore, cold cathode discharge tubes with Brewster windows and hollow cathodes similar to those of Reference 67. These discharge tubes will allow us to match the discharge conditions of Reference 53 and to reach the discharge energy densities of Reference 52.

We have attempted to detect the optogalvanic effect in H_2 discharges (Reference 67) so as to provide a reference for stabilization of the dye laser. Since these experiments were unsuccessful, we have examined the optogalvanic effect in our drift tube where we could control both the gas mixture and the E/n value. In nominally pure Ne with the E/n set for an electron multiplication of about 30, we observed an optogalvanic signal at the usual large number of Ne lines with a very good signal-to-noise ratio (1000) at the stronger lines. We then added H_2 so as to reduce the metastable lifetimes to about 10 μs as expected in H_2 (Reference 59) and obtained a signal to noise of about 2 at the Ne lines absorbed by $^3P_2$ metastables, but no signal at the other Ne lines. We have examined briefly the possibility of using mixtures of H_2 and NH_3 as a Penning mixture (Reference 25) so as to increase the optogalvanic effect in H_2. We saw no optogalvanic effect when we scanned through the spectral region appropriate to the transitions of Fig. 15.

SECTION IV

CONCLUSIONS

On the basis of the measurements and analyses described in this report we reach the following conclusions:

1) The infrared excitation transfer technique is a very useful method for the measurement of the coefficients for the vibrational excitation by electrons of homonuclear molecules, such as D_2, for which efficient infrared emitting molecules, such as CO_2 and CO, are in reasonably close energy resonance.

2) The excitation coefficients obtained from measurements in D_2-CO_2 mixtures are in good agreement with those obtained from D_2-CO mixtures when normalized to data from N_2-CO_2 and N_2-CO mixtures, respectively.

3) The coefficients for electron excitation of D_2 derived from our experiments are in good overall agreement with our calculated values, but show a somewhat slower variation with E/n than predicted using a cross section set adapted from the literature for D_2 and H_2. These data will have to be analyzed further to find a cross section set consistent with our excitation coefficients and published transport data for D_2.

4) Attempts to apply the excitation transfer technique in combination with an electron drift tube to the determination of vibrational excitation coefficients for H_2 by electrons were only marginally successful. To make measurements over a significant range of E/n it

would be necessary to find an infrared emitting molecule with a large excitation transfer rate coefficient and a high efficiency for radiation rather than quenching. The HCℓ molecule might satisfy these criteria.

5) Our measurements of the pressure dependence of the intensity of the near uv continuum emitted by H_2 molecules in the $a^3\Sigma_g^+$ state show a significantly larger quenching coefficient than do the previously published data. Also, at 300 K we see no evidence for collisional coupling to a nearby radiating state as previously reported for high temperature H_2.

6) Preliminary experimental efforts and analyses of published data suggest that in order to observe laser-induced fluorescence from the $c^3\Pi_u$ state of H_2 it will be necessary to use a gas discharge tube rather than our electron drift tube. The apparatus for these experiments has been constructed and a search for the fluorescence and the corresponding absorption has been initiated.

REFERENCES

1. D. Turnquist, R. Caristi, S. Friedman, S. Merz, R. Plante, and N. Reinhardt, IEEE Trans. Plasma Sci. PS-8, 185 (1980); M. Gundersen and S. Guha, J. Appl. Phys. 53, 1190 (1982).

2. A. Garscadden and W. F. Bailey, in Rarefied Gas Dynamics, edited by S. S. Fisher (Am. Inst. Aeronautics and Astronautics, 1981), Vol. 74, p. 1125; J. R. Hiskes, A. M. Karo, M. Bacal, A. M. Brunetau, and W. G. Graham, J. Appl. Phys. 53, 3469 (1982); M. Bacal, Physica Scripta T2/2, 467 (1982).

3. N. F. Lane, Rev. Mod. Phys. 52, 29 (1980).

4. J. N. Bardsley and J. M. Wadehra, Phys. Rev. 20, 1398 (1979).

5. G. J. Schulz, Rev. Mod. Phys. 45, 423 (1973).

6. For a recent summary of vibrational excitation cross section data in H_2, see: A. Klonover and U. Kaldor, J. Phys. B 12, 323 and 3797 (1979).

7. A. G. Engelhardt and A. V. Phelps, Phys. Rev. 131, 2115 (1963).

8. D. K. Gibson, Aust. J. Phys. 23, 683 (1970).

9. E. S. Chang and S.-F. Wong, Phys. Rev. Letters 38, 1327 (1977).

10. B. R. Bulos and A. V. Phelps, Phys. Rev. A 14, 615 (1976).

11. S. A. Lawton and A. V. Phelps, J. Chem. Phys. 69, 1055 (1978).

12. W. A. Rosser, Jr., A. D. Wood, and E. T. Gerry, J. Chem. Phys. 50, 4996 (1969).

13. J. C. Stephenson and C. B. Moore, J. Chem. Phys. 56, 1295 (1972).

14. W. H. Green and J. K. Handcock, J. Chem. Phys. 59, 4326 (1973).

15. T. Holstein, Phys. Rev. 72, 1212 (1947); 83, 1159 (1951). See also, M. Margottin-Maclou, L. Doyennette, and L. Henry, Appl. Opt. 10, 1768 (1971).

16. These transmission functions were empirical fits to curves obtained by differentiating numerically calculated equivalent widths from P. A. Jansson and C. L. Korb, J. Quant. Spectrosc. Radiat. Transfer 8, 1399 (1968).

17. S. S. Penner, Quantitative Molecular Spectroscopy and Gas Emissivities (Addison-Wesley, Reading, 1959), Chap. 8.

18. R. A. McClatchy, W. S. Benedict, S. A. Clough, D. E. Burch, R. F. Calfee, K. Fox, L. S. Rothman, and J. S. Garing, AFCRL Atmospheric Line Parameters Compilation, Air Force Cambridge Res. Lab. Report TR-73-0096 (unpublished); R. K. Huddelston, G. T. Fujimoto, and E. Weitz, J. Chem. Phys. 76, 3839 (1982); G. E. Caledonia, B. D. Green, and R. E. Murphy, J. Chem. Phys. 77, 5247 (1982).

19. D. Williams, D. C. Wenstrand, R. J. Brockman, and B. Curnutte, Molec. Phys. 20, 769 (1971); A. Picard-Bersellini, R. Charneau, and Ph. Brechignac, J. Chem. Phys. 78, 5900 (1983).

20. We have not found any data on the collisional broadening of the lines of the 4.3 μm band of CO_2 by H_2 or D_2 and so have used the data for broadening by N_2.

21. J. L. Moruzzi, J. W. Ekin, and A. V. Phelps, J. Chem. Phys. 48, 3070 (1968); F. C. Fehsenfeld, in Interactions Between Ions and Molecules, edited by P. Ausloos (Plenum, New York, 1975).

22. J. K. Theobald, J. Appl. Phys. 24, 123 (1953). When applying this formula, we used our calculated electron drift velocities and assumed that the electrons are emitted perpendicular to the cathode with an energy of 0.5 eV.

23. We find that it is necessary to lower electron excitation cross sections to obtain sufficient ionization in pure H_2 and D_2. For other sets of excitation cross sections for H_2, see: M. G. Heaps and A. E. S. Green, J. Appl. Phys. 46, 4718 (1975); P. Micheal and R. Winkler, Beit. Plasmaphysik 16, 233 (1976); H. Brunet and P. Vincent, J. Appl. Phys. 50, 4700 (1979); M. Cacciatore, M. Capitelli, and C. Gorse, J. Phys. D 13, 575 (1980).

24. Ionization coefficient data for H_2 is summarized by J. Dutton, J. Phys. Chem. Ref. Data 4, 577 (1975). Most measurements of ionization coefficients for D_2 are compared by C. G.-Morgan, W. D. Powell, and W. T. Williams, Brit. J. Appl. Phys. 18, 939 (1967).

25. H. Hotop, F. W. Lampe, and A. Niehaus, J. Chem. Phys. 51, 593 (1969).

26. D. A. Jennings, W. Braun, and H. P. Broida, J. Chem. Phys. 59, 4305 (1973).

27. M. Capitelli and M. Dilonardo, Chem. Phys. 24, 417 (1977).

28. J. R. Hiskes, J. Appl. Phys. 51, 4592 (1980).

29. D. W. Trainor, D. O. Hamm, and F. Kaufman, J. Chem. Phys. 58, 4599 (1973); K. P. Lynch, T. C. Schwab, and J. V. Micheal, Int. J. Chem. Kinetics 8, 651 (1976).

30. See, for example, R. T. Bailey and F. R. Cruikshank, in Gas Kinetics and Energy Transfer, edited by P. G. Ashmore and R. J. Donovan (Chemical Soc., London, 1978), Vol. 3.

31. A. V. Phelps and L. C. Pitchford (unpublished).

32. A. G. Engelhardt, A. V. Phelps, and C. G. Risk, Phys. Rev. 135, A1566 (1964); A. V. Phelps (unpublished).

33. A. J. Grimley and P. L. Houston, J. Chem. Phys. 70, 4724 (1979).

34. B. M. Hopkins and H.-L. Chen, J. Chem. Phys. 57, 3161 (1972).

35. J. Lukasik and J. Ducing, J. Chem. Phys. 60, 331 (1974); G. D. Billing, Chem. Phys. 20, 35 (1977).

36. H. Matsui, E. L. Resler, Jr., and S. H. Bauer, J. Chem. Phys. 63, 4171 (1975).

37. L. Doyennette, G. Mastrocinque, A. Chakroun, H. Gueguen, M. Margottin-Maclou, and L. Henry, J. Chem. Phys. 67, 3360 (1977).

38. C. B. Moore, R. E. Wood, B.-L. Hu, and J. T. Yardley, J. Chem. Phys. 46, 4222 (1967).

39. J. C. Stephenson, R. E. Wood, and C. B. Moore, J. Chem. Phys. 54, 3097 (1971).

40. W. A. Rosser, Jr. and E. T. Gerry, J. Chem. Phys. 54, 4131 (1971).

41. J. F. Bott, J. Chem. Phys. 65, 3921 (1976).

42. R. G. Miller and J. K. Handcock, J. Chem. Phys. 66, 5150 (1977).

43. The measurements of self relaxation of vibrationally excited H_2 are summarized by M. M. Audibert, C. Joffrin, and J. Ducing, Chem. Phys. Lett. 25, 158 (1974).

44. P. F. Zittle and C. B. Moore, Appl. Phys. Lett. 21, 81 (1972).

45. D. F. Starr, J. K. Handcock, and W. H. Green, J. Chem. Phys. 61, 5421 (1974).

46. A. J. Andrews and C. J. S. M. Simpson, Chem. Phys. Lett. 41, 565 (1976).

47. The self relaxation of vibrationally excited N_2 is summarized by R. L. Taylor and S. Bitterman, Rev. Mod. Phys. 41, 26 (1969).

48. The self relaxation of vibrationally excited CO at 290 K has been measured by M. G. Ferguson and A. W. Read, Trans. Faraday Soc. 61, 1559 (1965).

49. J. E. Land, J. Appl. Phys. 49, 5716 (1973).

50. W. S. Drozdoski, R. M. Young, R. D. Bates, Jr., and J. K. Handcock, J. Chem. Phys. 65, 1542 (1976).

51. G. Herzberg, Science of Light 16, 14 (1967).

52. D. S. Bethune, J. R. Lankard, and P. P. Sorokin, J. Chem. Phys. 69, 2076 (1978).

53. B. Dubreuil and A. Catherinot, J. Phys. 39, 1071 (1978).

54. K. A. Mohamed and G. C. King, J. Phys. B 12, 2809 (1979).

55. J. H. Breare and A. Von Engel, Proc. Roy. Soc. (London) A 282, 390 (1964).

56. R. E. Center, J. Chem. Phys. 54, 3499 (1971).

57. R. T. Thompson and R. G. Fowler, J. Quant. Spectrosc. Radiat. Transfer 12, 117 (1972).

58. T. J. Morgan, K.H. Berkner, and R. V. Pyle, Phys. Rev. A 5, 1591 (1972).

59. J. Godart and V. Puech, Chem. Phys. 46, 23 (1980).

60. R. P. Freis and J. R. Hiskes, Phys. Rev. A 2, 573 (1970); C. E. Johnson, Phys. Rev. A 5, 1026 (1972).

61. L.-Y. Chow Chiu, J. Chem. Phys. 70, 4376 (1979); B. Meierjohann and M. Volger, Phys. Rev. A 17, 47 (1978).

62. See, for example, K. K. Rohatgi-Mukherjee, Fundamentals of Photochemistry (Wiley, New York, 1978).

63. S.-I. Chu (private communication).

64. H. M. Crosswhite, The Hydrogen Wavelength Tables of Gerhard Heinrich Dieke (Wiley, New York, 19).

65. M. Glass-Maujean, J. Phys. Lett. 38, L-427 (1977).

66. W. Lichten, T. Wik, and T. A. Miller, J. Chem. Phys. 71, 2441 (1979).

67. D. Feldmann, Opt. Comm. 29, 67 (1979).

68. E. E. Eyler and F. M. Pipkin, Phys. Rev. Lett. 47, 1270 (1981); J. Chem. Phys. 77, 5315 (1982); Phys. Rev. A 27, 2462 (1983).

☆U.S. GOVERNMENT PRINTING OFFICE—759-062/800

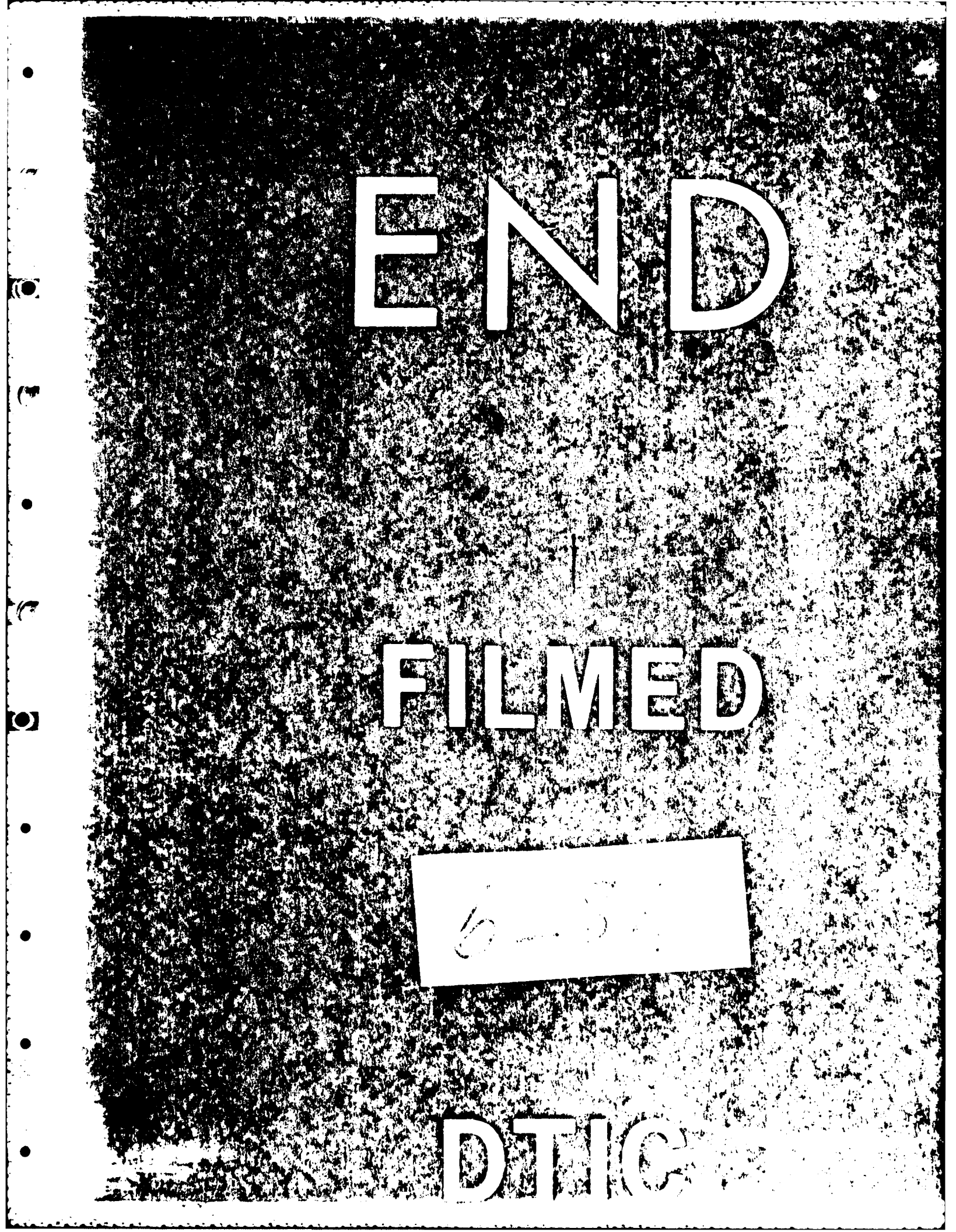
END
FILMED
DTIC